

NUREG/CR-1827
EGG-2072
Distribution category: R3

**LOSS-OF-COOLANT ACCIDENT
TEST SERIES—RESULTS OF
TC-1 TESTS**

Tom R. Yackle
Michael E. Waterman
Philip E. MacDonald

Published March 1981

EG&G Idaho, Inc.
Idaho Falls, Idaho 83415

Prepared for the
U.S. Nuclear Regulatory Commission
Washington, D.C. 20555
Under DOE Contract No. DE-AC07-76ID01570
FIN No. A6041

8104230462

ABSTRACT

The results of an in-pile nuclear blowdown test series, designated TC-1, are presented in this report. The primary objective of this test series was to investigate the influence of external cladding thermocouples on fuel rod thermal response during high pressure blowdown and subsequent low pressure reflood conditions. Results indicate that the presence of external cladding thermo-

couples slightly reduces local cladding temperatures by delaying the onset of critical heat flux, increasing cladding surface heat transfer, and promoting premature quench/rewet behavior. These results provide fundamental insight into the interpretation of results from previous in- and out-of-pile experiments in which external cladding thermocouples were included.

SUMMARY

A series of tests has been conducted in the Power Burst Facility (PBF) at the Idaho National Engineering Laboratory to evaluate the influence of external cladding thermocouples on the thermal and mechanical behavior of nuclear fuel rods during loss-of-coolant accident (LOCA) conditions. These tests were performed with four Loss-of-Fluid Test (LOFT) type fuel rods contained in individual flow shrouds. The fuel rods were symmetrically positioned within a test train in the PBF in-pile tube in an environment similar to the LOFT experiment environment. Two rods were instrumented with four LOFT cladding surface thermocouples, with junctions located near the high power region of the fuel rods. The external thermocouples were extended to the bottom of the fuel stack with dummy thermocouple wires. All four rods were instrumented with internal thermocouples, with junctions at the same axial elevation as the external thermocouples. The internal thermocouples were fitted in slots on the surface of the fuel pellets. Some of the thermocouple junctions were welded directly to the inside cladding surface and the remainder were fitted into holes near the surface of the fuel pellets. By comparing the response of internal thermocouples, the behavior of fuel rods with and without external thermocouples during a LOCA was examined.

The TC-1 Test Series consisted of four LOCA transients. Each test was subdivided into power calibration, decay heat buildup, blowdown, heatup, and reflood phases. The system conditions at the initiation of each blowdown were approximately 600 K inlet temperature, 15.5 MPa system pressure, and 49.5 kW/m maximum rod power. Each test was designed to simulate the LOFT L2 experiments as closely as possible. To simulate LOFT conditions, the TC-1 tests included (a) a system depressurization that was similar to LOFT, (b) preprogrammed rod powers to achieve blowdown cladding peak temperatures of about 1000 K, (c) preprogrammed hot and cold leg valve sequencing that resulted in a two-phase liquid slug forced past each fuel rod early in blowdown to simulate the rod quench measured during the LOFT experiments, and (d) a reflood rate to simulate the core reflooding that occurred in LOFT.

On the basis of the TC-1 tests, surface thermocouples were found to influence the fuel rod

cladding temperatures during both the blowdown and reflood phases of a LOCA. During blowdown, the surface thermocouples caused a delay in the initial occurrence of critical heat flux (CHF) and improved the cladding surface heat transfer, subsequently reducing the cladding temperatures. Peak temperatures measured during blowdown were generally about 60 K lower for each second of delay in CHF. An additional reduction in measured peak temperatures of about 50 K apparently resulted from the improved cladding heat transfer due to the surface thermocouples.

The measured cladding quench times and subsequent rewet times also varied, with the TC-1 fuel rods with external thermocouples quenching from 3 to 12 s before the other rods. In addition, some external thermocouples did not properly measure the cladding temperature response, as was evident by the momentary quenching and reheating of the thermocouple prior to the actual rod quench. The momentary quenching of the TC-1 external thermocouples apparently occurred as precursory cooling selectively quenched the thermocouple prior to the arrival of the cladding quench front.

Determination of thermocouple effects during the TC-1 tests required similar thermal-hydraulic conditions within the flow shrouds of the four test rods. Unfortunately, some shroud coolant leakages were found after TC-1 that could have influenced the fuel rod cladding temperature data. Total shroud leakages of Rods 01 and 04, the two rods without external thermocouples, were similar; however, the thermocouple data indicated that the Rod 04 temperatures may have been slightly reduced and the time-to-CHF slightly increased by the leakages. The shroud leakage of Rod 03, a rod with external thermocouples, was less than the other test rods; therefore, the comparison of thermocouple data between this rod and Rods 01 and 04 is valid. Finally, a cracked shroud weld of Rod 02, a rod with external thermocouples, was shown to have significantly influenced the cladding temperatures during three of the four TC-1 transients. The data for this rod during these transients have not been considered in the conclusions of this report.

An attempt was made during the TC-1 tests to simulate the LOFT L2-2 and L2-3 blowdown conditions in which a two-phase coolant slug was

forced past the fuel rods during the early portion of blowdown. Understanding the effects of external thermocouples during the LOFT L2 experiments, with a core rewet, is extremely important in interpreting the LOFT data. Generally, all the TC-1 thermocouples measured rod cooling during the slug period, but the cladding did not quench as measured during the LOFT L2 experiments. The two-phase slug apparently consisted of high quality vapor that could not rapidly quench the TC-1 rods. To more closely simulate LOFT conditions, the liquid content of the two-phase slug should be increased. A means of attaining this condition in the PBF has been established and a second test series, TC-3, is planned to investigate possible thermocouple effects during a blowdown quench.

The LOFT L2 data and results of similar programs can be adjusted on the basis of the TC-1 results. The thermocouples used in the LOFT L2 experiments measured CHF from 1 to 1.6 s after blowdown initiation. If CHF occurred between 0.5 and 1.0 s earlier on rods without cladding surface thermocouples, then the cladding peak temperatures could have been 30 to 60 K higher. The cladding thermocouples may have also enhanced the surface heat transfer and reduced the cladding peak temperature of the rods instrumented with

surface thermocouples. Assuming the TC-1 results are applicable, the rods with cladding thermocouples may be cooler (by about 50 K) than uninstrumented rods, due to enhanced surface heat transfer associated with the external thermocouples. Therefore, the peak temperatures of the LOFT fuel rods with external thermocouples may have been between 80 and 110 K lower than adjacent, uninstrumented rods.

The TC-1 rods with surface thermocouples also quenched between 3 and 12 s earlier than the rods without surface thermocouples during the 4-cm/s reflood. On the basis of these results, it is possible that during the LOFT L2-2 and L2-3 experiments, the rods without surface thermocouples may have quenched somewhat later than rods with surface thermocouples. In addition, some of the TC-1 surface thermocouples did not measure the true cladding temperature response (by momentarily quenching and reheating prior to actual rod quench), a condition that has apparently occurred in other test programs. Finally, all the fuel and cladding thermocouples performed exceptionally well during the TC-1 tests. Future in-pile programs should consider internal rod temperature measurements in place of surface temperature measurements.

ACKNOWLEDGMENTS

The authors wish to thank Dr. R. Van Houten (Nuclear Regulatory Commission) for his design recommendations and support of the TC-1 Test

Series, and Mr. Ed Courtwright and his associates at Battelle Pacific Northwest Laboratory for the fabrication of the four TC-1 fuel rods.

CONTENTS

ABSTRACT	ii
SUMMARY	iii
ACKNOWLEDGMENTS	v
INTRODUCTION	1
TC-1 THERMAL-HYDRUALICS	3
System Depressurization	3
Fuel Rod Shroud Coolant Flow	3
FUEL ROD THERMAL AND MECHANICAL RESPONSE	6
Behavior of Rod 01	6
Behavior of Rod 02	9
Behavior of Rod 03	9
Behavior of Rod 04	13
COMPARISON OF SELECTED RESULTS	16
Comparison of Selected Internal Cladding and Fuel Surface Temperatures During Test TC-1A	16
Comparison of LVDT and Internal Temperature Results During Blowdown	16
Comparison of Selected Results During Reflood	25
CONCLUSIONS	28
REFERENCES	29
NOTE: All of the appendices to this report are presented on microfiche attached to the inside of the back cover.	
APPENDIX A—ADDITIONAL PLOTS FOR TESTS TC-1B, TC-1C, AND TC-1D	37
APPENDIX B—THERMAL-HYDRAULIC DATA RELATED TO TC-1 TESTS	71
APPENDIX C—FUEL ROD CHARACTERIZATION	79
APPENDIX D—EXPERIMENT DESIGN AND CONDUCT	87

FIGURES

1. Cold leg depressurization during Test TC-1A	4
--	---

2.	Flow shroud outlet volumetric flow rates of Rods 01, 02, and 03 during Test TC-1A	4
3.	Flow shroud inlet volumetric flow rates of all rods during Test TC-1A	5
4.	Internal temperatures of Rod 01 during Test TC-1A	7
5.	Internal temperatures and cladding axial displacement of Rod 01 during Test TC-1C	7
6.	Internal temperatures and cladding axial displacement of Rod 01 during blowdown phase of Test TC-1C	8
7.	Internal temperatures and cladding axial displacement of Rod 01 during reflood phase of Test TC-1C	8
8.	Rod internal and cladding surface temperatures, and cladding axial displacement of Rod 02 during Test TC-1A	10
9.	Rod internal and cladding surface temperatures, and cladding axial displacement of Rod 02 during blowdown phase of Test TC-1A	10
10.	Rod internal and cladding surface temperatures, and cladding axial displacement of Rod 02 during reflood phase of Test TC-1A	11
11.	Rod internal and cladding surface temperatures, and cladding axial displacement of Rod 03 during Test TC-1A	12
12.	Rod internal and cladding surface temperatures, and cladding axial displacement of Rod 03 during blowdown phase of Test TC-1A	12
13.	Rod internal and cladding surface temperatures, and cladding axial displacement of Rod 03 during reflood phase of Test TC-1A	13
14.	Rod internal temperatures and cladding axial displacement of Rod 04 during Test TC-1A	14
15.	Rod internal temperatures and cladding axial displacement of Rod 04 during blowdown phase of Test TC-1A	14
16.	Rod internal temperatures and cladding axial displacement of Rod 04 during reflood phase of Test TC-1A	15
17.	Comparison of internal cladding temperatures of Rods 01 and 02 during Test TC-1A	17
18.	Comparison of internal fuel temperatures of Rods 01 and 02 during Test TC-1A	17
19.	Comparison of internal fuel temperatures of Rods 01 and 03 during Test TC-1A	18
20.	Comparison of internal fuel temperatures of Rods 03 and 04 during Test TC-1A	18
21.	Comparison of cladding axial displacement measurements during Test TC-1A	19
22.	Comparison of cladding axial displacement measurements during Test TC-1B	19
23.	Comparison of cladding axial displacement measurements during Test TC-1C	20

24.	Comparison of cladding axial displacement measurements during Test TC-1D	20
25.	Comparison of internal fuel and cladding temperatures of Rod 01 during Test TC-1A	22
26.	Comparison of internal fuel and cladding temperatures of Rod 02 during Test TC-1A	22
27.	Comparison of Rod 03 internal fuel temperatures during Test TC-1A	23
28.	Comparison of Rod 04 internal fuel temperatures during Test TC-1A	23
29.	Comparison of blowdown cladding peak temperatures with time-to-CHF during TC-1 tests	24
30.	Comparison of all internal rod temperatures during reflood phase of Test TC-1A	26
31.	Comparison of all internal rod temperatures during reflood phase of Test TC-1B	26
32.	Comparison of all internal rod temperatures during reflood phase of Test TC-1C	27
33.	Comparison of all internal rod temperatures during reflood phase of Test TC-1D	27

TABLE

1.	Comparison of CHF times for all TC-1 rods	21
----	---	----

LOSS-OF-COOLANT ACCIDENT TEST SERIES—RESULTS OF TC-1 TESTS

INTRODUCTION

Several criteria must be satisfied before a light water reactor (LWR) operating license can be granted. One of these criteria is that the predicted behavior of the reactor during a postulated loss-of-coolant accident (LOCA) must conform to restrictions imposed by the Code of Federal Regulations.¹ To ensure that the actual behavior of both the cooling system and the nuclear core is accurately predicted in computer codes, in-pile experiments, which provide data for the development and improvement of existing computer code models, are being conducted in the Loss-of-Fluid Test (LOFT)² Facility and in the Power Burst Facility (PBF).³ The LOFT Facility was designed to represent the behavior of a large pressurized water reactor (PWR) during a postulated LOCA. The PBF LOCA program is one of several programs that are providing in-pile information on the behavior of nuclear fuel rods subjected to normal, off-normal, and accident conditions.

In the LOFT and PBF tests, the fuel rod cladding temperature data have been obtained with thermocouples welded to the cladding outer surface. These data are used to assess the accuracy of computer models that predict cladding temperature response, and to evaluate and interpret test train thermal-hydraulic behavior. The cladding surface thermocouples, however, may be acting as cooling fins and local sites of cladding rewet, and, hence, may be influencing fuel rod thermal behavior.

The influence of cladding surface thermocouples on fuel rod behavior during a LOCA is currently being investigated at several facilities. The majority of these investigations are being conducted in out-of-pile tests with simulated nuclear fuel rods. Blowdown experiments were recently conducted at the EG&G Idaho, Inc., LOFT Test Support Facility with a single heater rod subjected to conditions designed to simulate the rewet of a nuclear fuel rod during blowdown and reflood. Significant differences in rod quench times were measured between rods with and without surface thermocouples. A series of out-of-pile blowdown

experiments are also currently being conducted at the Karlsruhe Cosima blowdown facility in Germany to investigate the effects of surface thermocouples. A preliminary series of blowdown tests⁴ are complete, and significant temperature differences between electric rods with and without the simulated LOFT thermocouples have been measured. Future tests are also scheduled with actual LOFT thermocouples to better quantify these differences.

The EG&G Idaho, Inc., LOFT Program has also conducted a series of transient (blowdown) critical heat flux (CHF) tests⁵ at the Columbia University Chemical Engineering Research Laboratory. The purpose of these tests was to evaluate the effects of cladding surface thermocouples on the time-to-CHF and to develop a CHF correlation appropriate for use in LOFT. Two electrically heated 25-rod bundles simulating a portion of the LOFT nuclear reactor core were tested. The tests were conducted as simultaneous hot and cold leg break LOCAs, in which coolant stagnation and CHF occurred rapidly. The maximum difference in time-to-CHF between bundles with and without surface thermocouples was less than 0.45 s, and most differences were less than 0.20 s. An analysis of the behavior of a hot fuel rod during the LOFT L2-4 experiment indicated that a difference in CHF of 1 s could result in a 52-K difference in surface peak temperature. It was therefore concluded that surface thermocouples were not significantly influencing the blowdown cladding peak temperatures in LOFT.

A number of other experiments are currently being conducted to investigate thermocouple effects during reflood. These experiments are being conducted in the Halden reactor in Norway,⁶ the Swiss Reflood Facility, the University of California at Los Angeles (UCLA), and the Rebeka Reflood test facility in Germany. Final results of these experiments are currently unavailable; however, preliminary results from the UCLA tests show that external thermocouples enhance cladding quench and that the quench

front travels up the thermocouple sheath faster than it travels up the cladding. Steam with entrained liquid generated during reflood tended to quench downstream surface thermocouples and the adjacent cladding prior to the actual quench front.

The results of a series of in-pile tests conducted in the Power Burst Facility to specifically evaluate the influence of cladding surface thermocouples on nuclear fuel rod thermal and mechanical behavior during PBF LOCA conditions are reported in this document. These tests were performed with four LOFT-type fuel rods contained in individual flow shrouds. The fuel rods were symmetrically positioned within a test train in the PBF in-pile tube.

Fuel rod instrumentation for the TC-1 tests consisted of a linear variable differential transformer (LVDT) at the bottom of each fuel rod to measure cladding axial displacement, and cladding and fuel thermocouples located near the high power region of each rod. Twelve internal rod thermocouples were fitted in slots on the outer surface of the fuel stacks (three per rod). Eight of these thermocouples had junctions located in small holes near the surface of the fuel pellets to measure fuel surface temperatures. The four remaining thermocouples had junctions welded to the inner surface of the cladding of two of the four fuel rods to measure internal cladding surface temperatures. Additionally, two of the fuel rods were externally instrumented with four LOFT-type cladding surface thermocouples, with junctions located at the same axial elevation as the internal thermocouple junctions.

Four LOCA transients were conducted during the TC-1 series. Test TC-1A consisted of a power

calibration and fuel preconditioning phase, and, as in Tests TC-1B, TC-1C, and TC-1D, a decay heat buildup phase followed by blowdown, heatup, and reflood phases. The four tests were designed to simulate the LOFT L2 experiments as closely as possible, with initial system conditions of approximately 600 K inlet coolant temperature, 15.5 MPa system pressure, 0.8 L/s inlet flow rate, and 49.5 kW/m rod peak power. As in the LOFT experiments, the cladding temperatures reached about 1000 K during the transient phase of the tests. Five to seven seconds after initiation of blowdown, a two-phase liquid slug was forced past the fuel rods for varying time periods (2 to 6 s, depending on the test) to simulate the LOFT L2-2 and L2-3 cooling that occurred during blowdown. Finally, the fuel rods were quenched during the reflood portion of the tests at conditions that best simulated a LOFT L2 reflood in the PBF.

A discussion of the TC-1 thermal-hydraulics and the thermal and mechanical response of the fuel rods, as well as a comparison of selected results are presented, followed by a discussion of the conclusions derived from the test series. The data presented in this report have not been fully qualified with normal corrections and offsets. A complete set of data for Tests TC-1B, TC-1C, and TC-1D is provided in Appendix A (Test TC-1A is discussed extensively within the report). Thermal-hydraulic and fuel rod characterization data are provided in Appendices B and C, respectively. The design of the Test TC-1 test train and PBF blowdown system and the test conduct are described in Appendix D. (All of the appendices to this report are presented on microfiche attached to the inside of the back cover.)

TC-1 THERMAL-HYDRAULICS

The thermal-hydraulic response of the TC-1 tests is characterized by the system depressurization and the volumetric flow within each fuel rod flow shroud. Test TC-1A results were selected for discussion in this section. A complete set of experimental measurements from the other three tests (Tests TC-1B, TC-1C, and TC-1D) are provided in Appendix A.

System Depressurization

The measured coolant depressurization during Test TC-1A is shown in Figure 1. After closing the warmup line prior to blowdown, the coolant in the cold leg was subcooled and essentially incompressible at conditions of about 595 K and 15.5 MPa. The PBF primary coolant loop was isolated from the in-pile tube and blowdown system at time zero. Both cold leg blowdown valves were opened at 0.1 s, and subcooled depressurization began as the coolant was rapidly expelled through the converging-diverging nozzles. This phase of depressurization lasted approximately 0.1 s, followed by coolant flashing and choked two-phase flow in the converging-diverging nozzles, which limited the decompression rate. The large (23.9 mm) cold leg valve was closed between 4 and 22 s to further reduce the depressurization rate so that the entire depressurization would be similar to that in the LOFT L2 experiments. The system was fully depressurized within about 27 s.

Fuel Rod Shroud Coolant Flow

The fuel rod coolant volumetric flow response was measured at the shroud outlet (upper turbine meters) and shroud inlet (lower turbine meters) and is shown in Figures 2 and 3. The outlet volumetric flow rates shown in Figure 2 rapidly decreased from 0.8 L/s to zero at initiation of the blowdown transient due to the closure of the check valves. Since the flow was negative for most of the blowdown, the check valves remained closed and the shroud outlet flow was near zero (except from 7 to 9 s when the blowdown valves were cycled). A comparison of the upper turbine volumetric flows for Rods 01, 02, and 03 shows that the flow was essentially the same in all of the shrouds, as expected. The Rod 04 upper turbine

did not function. Between 7 and 9 s, one hot leg valve was opened and the cold leg valve closed to force a two-phase slug of liquid from the lower plenum and downcomer upward past the fuel rods. The resultant two-phase slug reached a peak flow rate of 1.0 L/s during this period. The PBF cold and hot leg valves were then recycled at 9 s to close the check valves and terminate the slug phase. Reflood was initiated at 100 s with a brief period of high flow reflood (1.6 L/s) to fill the lower plenum, followed by low flow reflood (0.95 L/s) until the rods rewet. The outlet volumetric flow was positive during reflood and oscillated as reflood water quenched the cladding. Cladding rewet was completed at about 125 s as the outlet volumetric flow rate became equal to the inlet volumetric flow rate and single-phase liquid filled each shroud.

The lower turbine volumetric flow within each shroud during Test TC-1A is presented in Figure 3. The volumetric flow became negative as the test was initiated and remained negative during the early stages of blowdown. Cycling of the hot and cold leg blowdown valves between 7 and 9 s resulted in the two-phase slug period with a maximum positive flow rate of 0.7 L/s, similar to the outlet turbines. The valves were recycled at 9 s to reestablish downward flow through the shroud inlet to the cold leg. The flows gradually decreased to about 0.1 L/s at 20 s. The large cold leg blowdown valve was reopened at 22 s, and the lower turbine volumetric flow increased (became more negative) at this time. The reason for this increase is not completely understood, but it may be associated with an increased pressure drop across the check valve and shroud and a slight leakage of steam through the shroud leakage paths. However, the increase in inlet volumetric flow at 22 s may also be associated with expansion of the steam within the flow shrouds. The depressurization was completed by about 27 s and the volumetric flow was essentially zero between 50 and 100 s in all shrouds. After 100 s, the flow oscillated as reflood water entered the flow shrouds.

The positive volumetric flow spike at the inlet during the two-phase slug period was nearly identical with the outlet volumetric flow spike. However, as coolant was forced past the fuel rods, the volumetric flow should have significantly

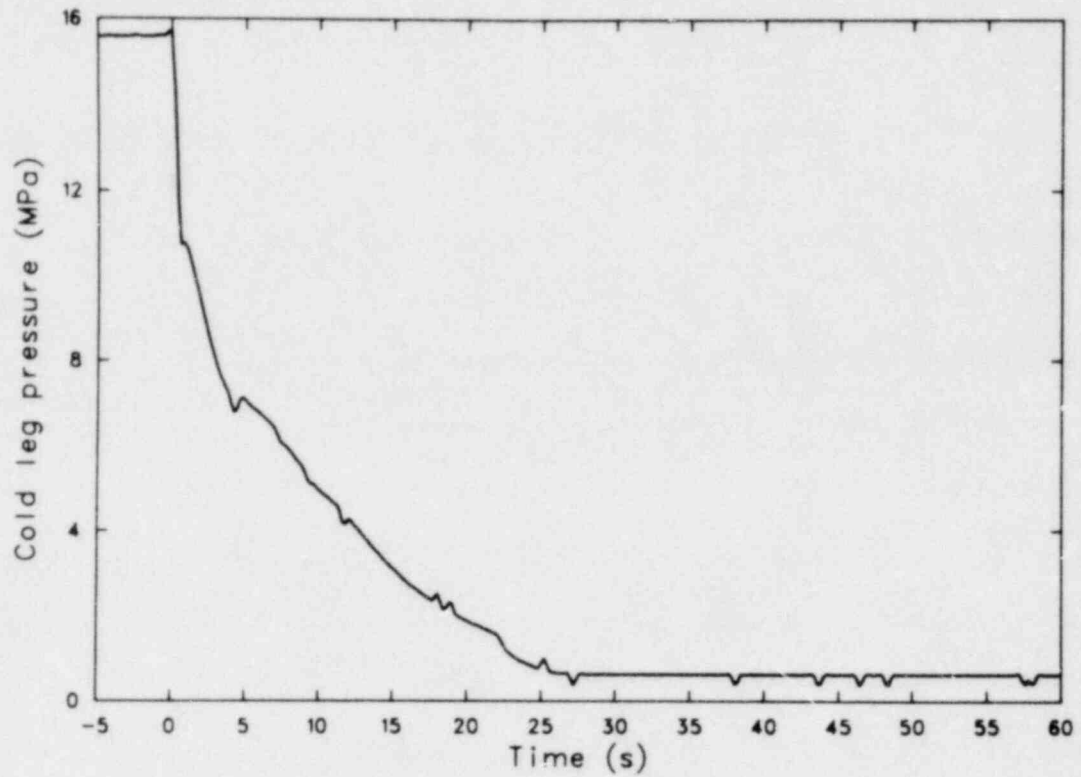


Figure 1. Cold leg depressurization during Test TC-1A.

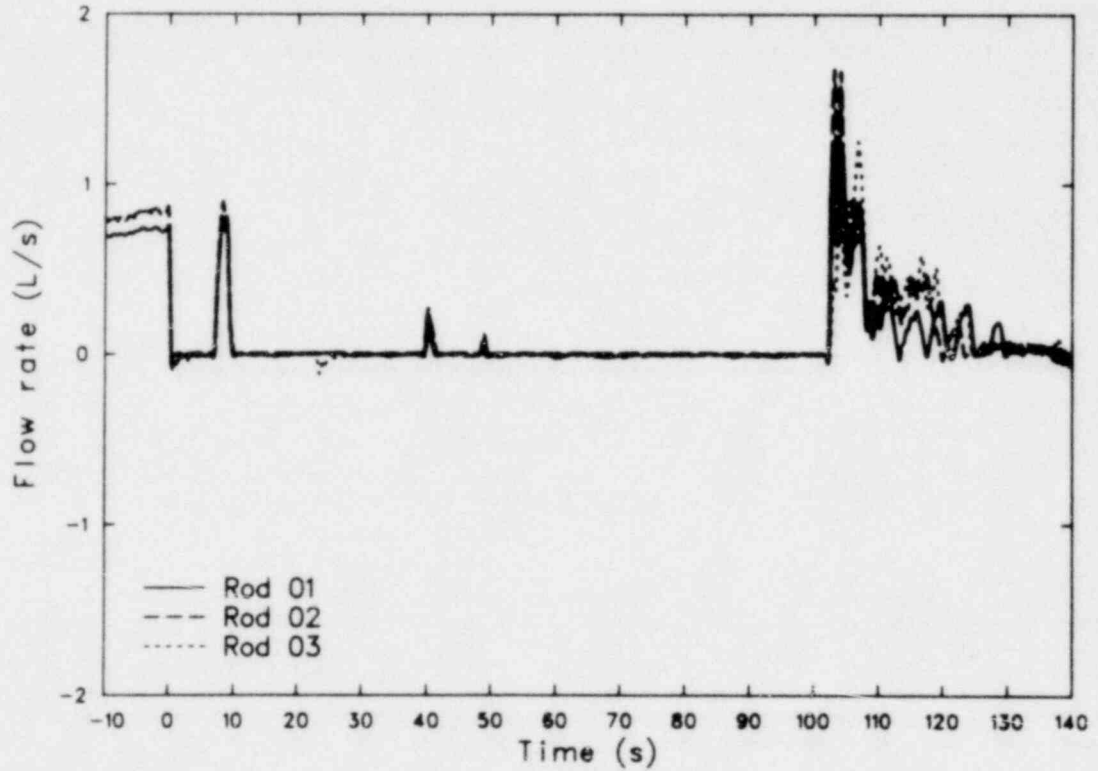


Figure 2. Flow shroud outlet volumetric flow rates of Rods 01, 02, and 03 during Test TC-1A.

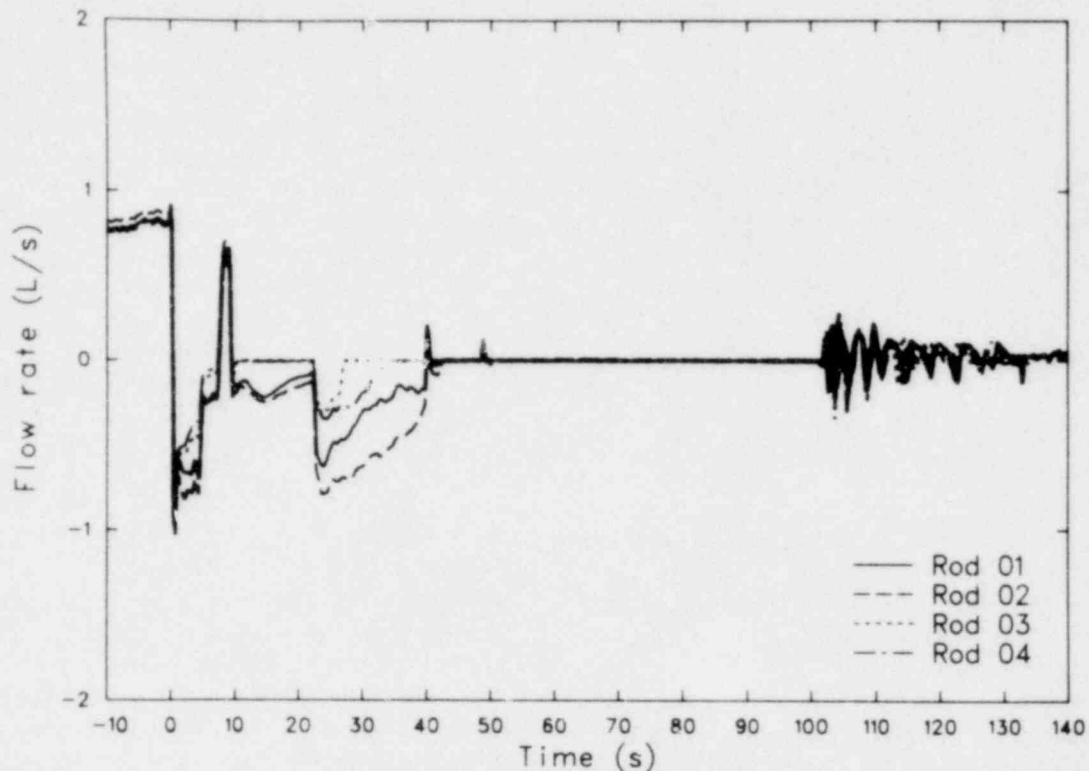


Figure 3. Flow shroud inlet volumetric flow rates of all rods during Test TC-1A.

increased from inlet to outlet as the coolant enthalpy increased. Since the flows measured by the inlet and outlet turbines were similar, the slug flow through the shrouds apparently had little effect on the fuel rod stored energy and temperatures. This conclusion is verified by the fuel rod thermocouple measurements presented in the next section.

The responses of the four inlet turbine meters during blowdown provide a measurement of the relative degree of flow shroud leakage. The inlet volumetric flows of the four test rods were generally similar during Test TC-1A, with the largest measured flow past Rod 02. The Rod 02 shroud leakage apparently increased after the first blowdown since the volumetric flow at the shroud inlet became significantly larger during Tests TC-1B, TC-1C, and TC-1D compared with TC-1A. These unexpectedly large flows resulted from leakage of coolant, during blowdown, from

the bypass region into the flow shroud through a cracked weld (discussed in Appendix D) in the upper portion of the shroud. The weld probably failed (or the failure became significantly larger) after the first test. The Rod 01 inlet volumetric flow was consistently the third largest of the four shrouds, but this rod reached the highest temperatures. A cracked weld was also found in the upper portion of the Rod 01 shroud; however, the leakage through this crack apparently did not significantly influence the rod thermal response. The Rod 01 weld failure probably occurred during or after Test TC-1D. The inlet volumetric flows of the other rods were similar during each TC-1 transient. On the basis of these results, the unexpectedly large flows past Rod 02 during Tests TC-1B, TC-1C, and TC-1D probably influenced the cladding temperature and time of CHF. Therefore, the Rod 02 data from Tests TC-1B, TC-1C, and TC-1D are not considered in this report during blowdown. Data from this rod (in all tests) are still applicable during reflood.

FUEL ROD THERMAL AND MECHANICAL RESPONSE

The thermal and mechanical response of each rod during Test TC-1A (and limited results of Test TC-1C) is summarized. Data from selected internal and external thermocouples and the linear variable differential transformers (LVDTs) of each fuel rod are presented. Thermocouple data not presented in this section substantiate the trends of the thermocouple data selected for presentation.

Behavior of Rod 01

The Tests TC-1A and TC-1C data from one internal cladding and one fuel thermocouple and the LVDT^a (Test TC-1C only) on Rod 01, a rod without external thermocouples, are presented in Figures 4 and 5. The LVDT did not function properly during Tests TC-1A and TC-1B. The fuel and internal cladding temperatures at the thermocouple locations were 1128 and 855 K, respectively, prior to the Test TC-1A blowdown transient. Similar temperatures were measured prior to the Test TC-1C blowdown (1030 and 810 K, respectively). During the first second of each TC-1 blowdown, both the fuel and internal cladding temperatures gradually decreased until CHF occurred at about 0.8 to 0.9 s, and then rapidly increased until about 7 s when the blowdown two-phase slug passed the rods. A rewet of the cladding occurred during Test TC-1C at about 1.5 s, which momentarily reduced the internal cladding temperature to about 800 K. The Rod 01 internal temperatures during Test TC-1A (Figure 4) reached a maximum value at about 7 s and then decreased by about 60 K between 7 and 9 s, the time of the two-phase slug injection. In comparison, the measured temperatures during Test TC-1C (Figure 5) decreased by about 190 K between 5 and 11 s, the time of the two-phase slug injection. The reactor operator intentionally adjusted the core power after 20 s to establish cladding temperatures at about 1000 to 1100 K prior to reflood.

a. The LVDT measured the relative change in length of the fuel rod and flow shroud. When the data are corrected for the shroud thermal expansion and the effects of the instrument temperature sensitivity, the general shape of the LVDT curves corresponds well with that of the thermocouple.

The LVDTs used in the TC-1 tests primarily responded to the axial extension or elongation of the cladding and provided an indication of the average cladding temperature. The Rod 01 LVDT (Figure 5) measured a cladding extension following CHF, within the first second of blowdown, and a continued elongation until the two-phase slug period. As the rod gradually cooled during the slug period, the LVDT measured a decrease in the Rod 01 elongation. This trend reversed after 11 s as the cladding continued to heat until about 50 s.

The fuel rod gradually cooled during the two-phase slug period early in the transient rather than rapidly quenching as observed in the LOFT L2 experiments. The gradual cooling during the TC-1 tests was apparently caused by the flow of high quality vapor past the fuel rods. In comparison, the coolant quality in the LOFT core during the blowdown quench has been estimated to be between 0 and 30%. Therefore, the hydraulic conditions of the two-phase slug during the TC-1 tests did not accurately represent the conditions that occurred in LOFT.

Details of the Rod 01 thermal response during the blowdown phase of Test TC-1C are presented in Figure 6. Critical heat flux was measured at 0.9 s by both internal thermocouples and the LVDT. The internal cladding thermocouple indicated the occurrence of a momentary rewet between 1 and 2 s, a phenomenon previously observed in PBF LOCA tests. The internal cladding thermocouple that indicated the momentary rewet was welded to the inner surface of the cladding. Similar rewets were not measured by the fuel thermocouples located near the outer surface of the pellets of this rod, indicating that the fuel and cladding thermal behavior were apparently decoupled during the momentary quench.

Details of the Rod 01 thermal response during the reflood phase of Test TC-1C are presented in Figure 7. The rod thermal response during reflood can be divided into several time periods. First, a relatively slow temperature decrease of approximately 15 K/s occurred between about 104 and 115 s. This decrease was associated with gradual oscillations of the cladding temperature as precursory cooling passed along the hot cladding. After about 115 s, the internal thermocouples measured

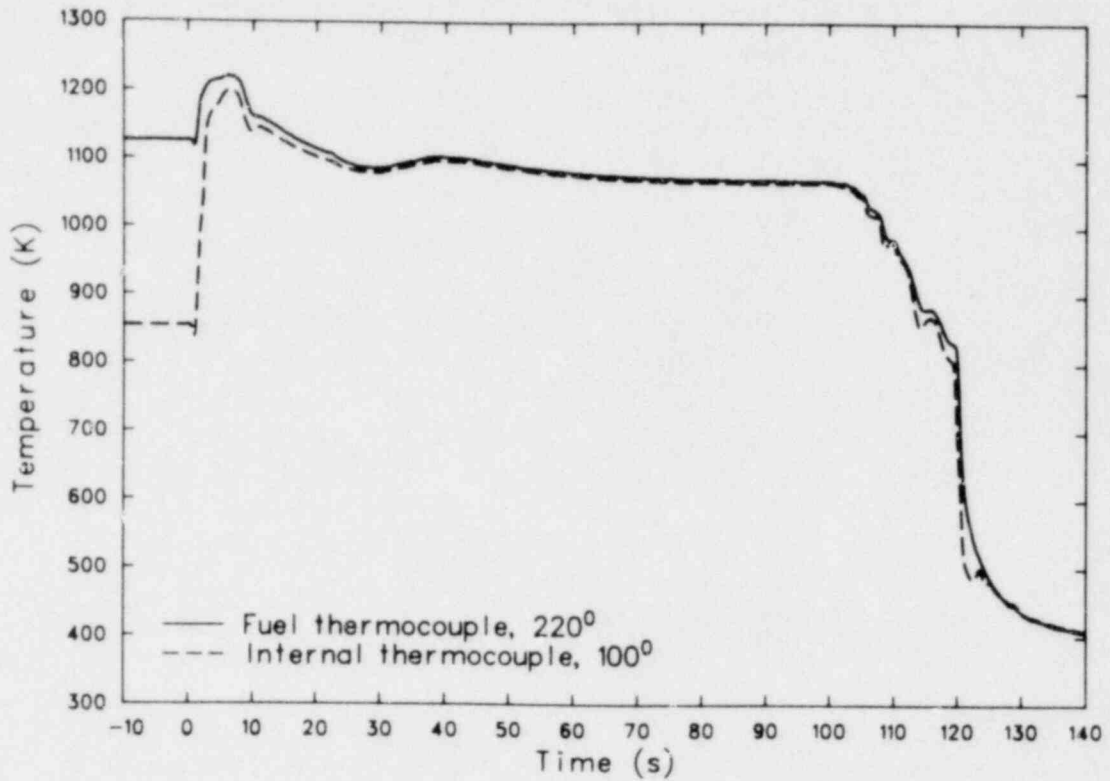


Figure 4. Internal temperatures of Rod 01 during Test TC-1A.

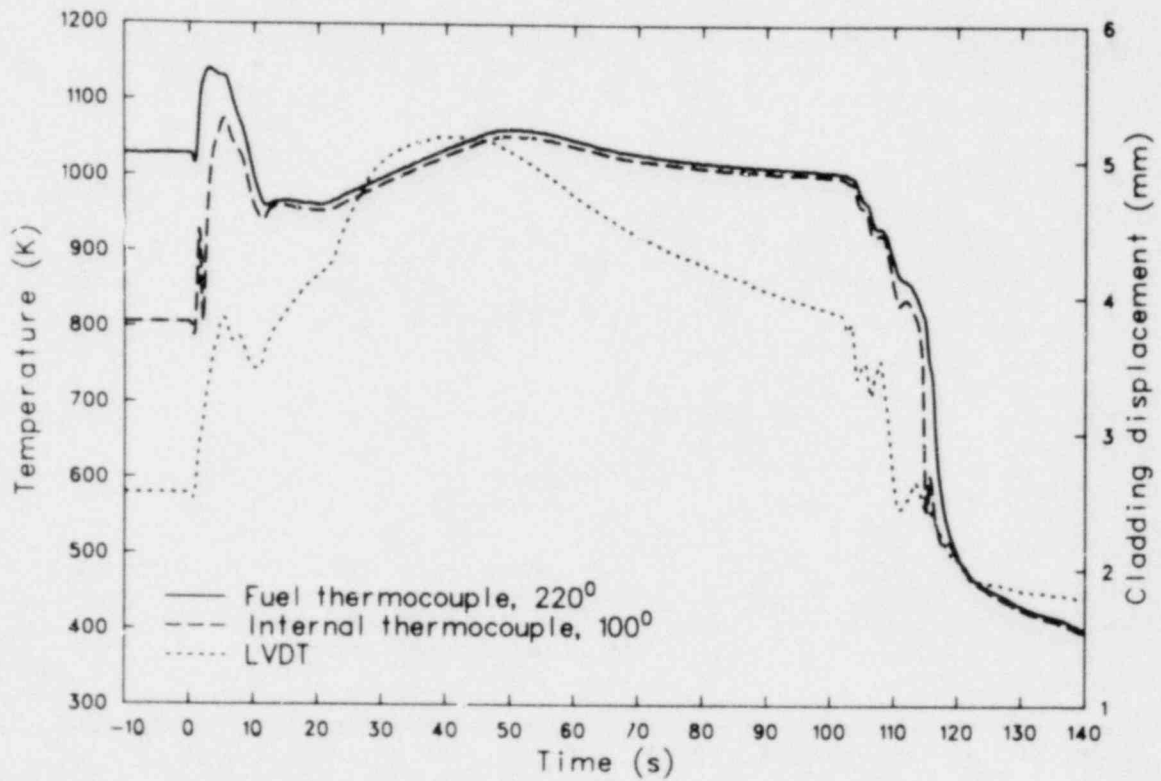


Figure 5. Internal temperatures and cladding axial displacement of Rod 01 during Test TC-1C.

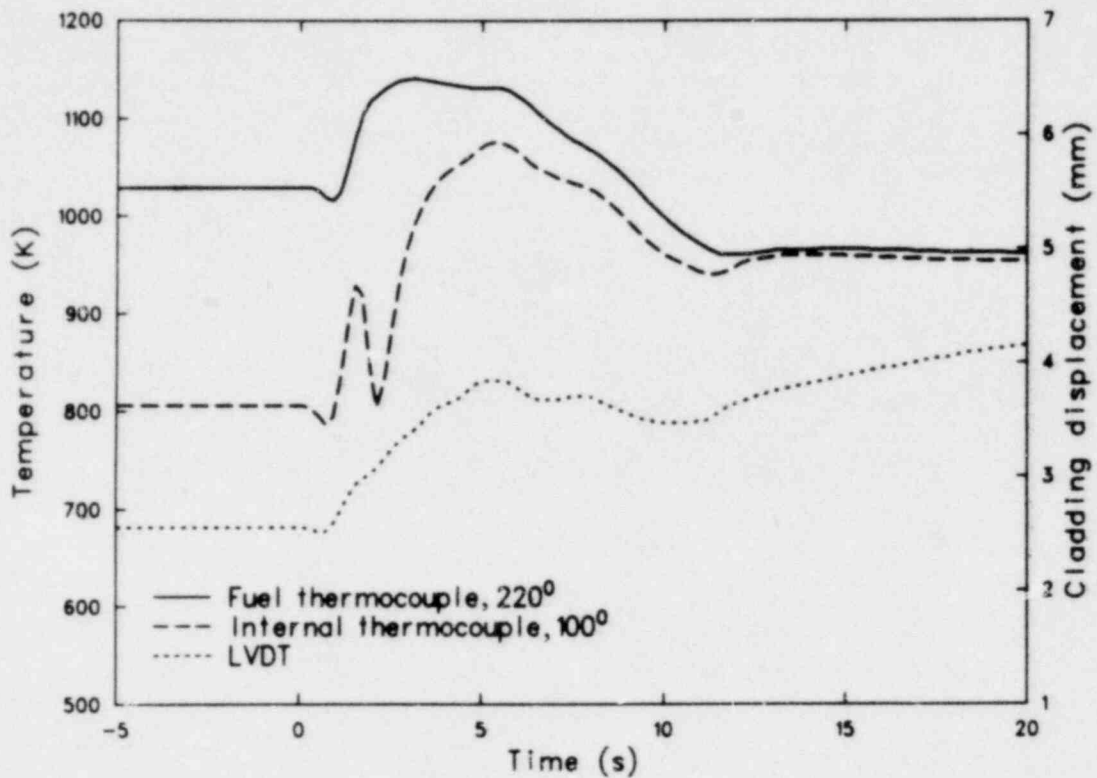


Figure 6. Internal temperatures and cladding axial displacement of Rod 01 during blowdown phase of Test TC-1C.

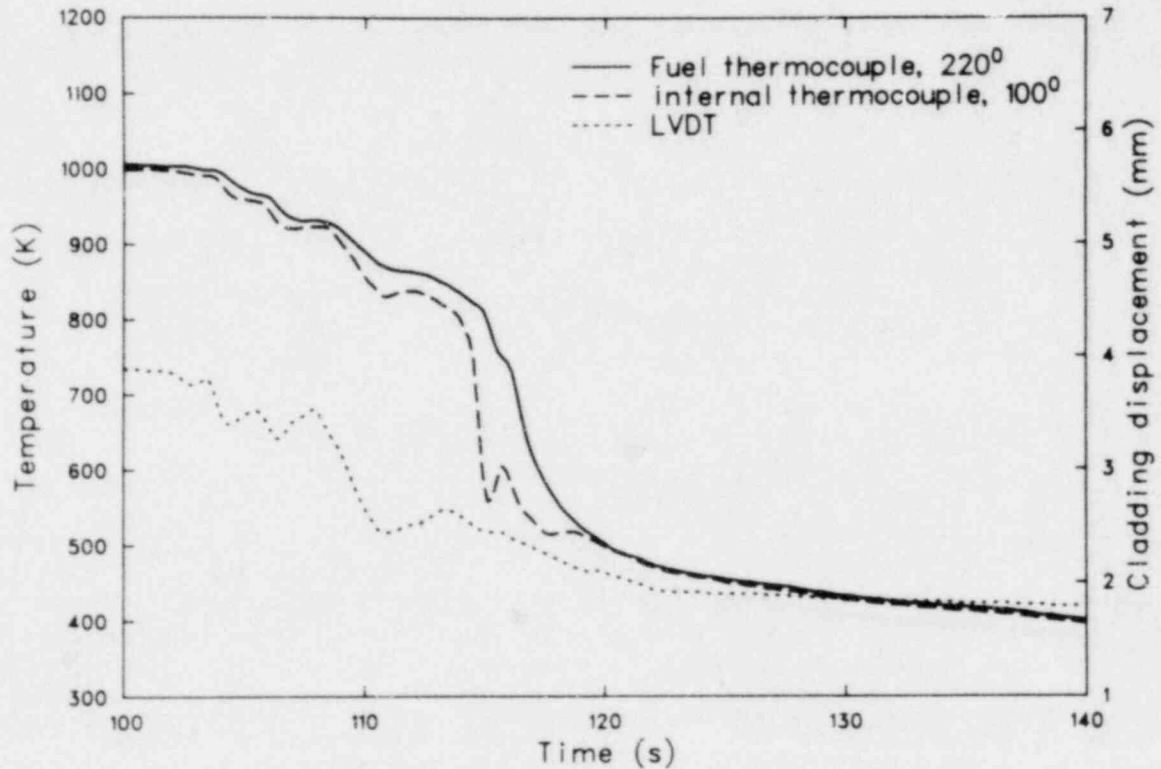


Figure 7. Internal temperatures and cladding axial displacement of Rod 01 during reflood phase of Test TC-1C.

cladding quench (a rapid temperature decrease). The cladding surface heat transfer must have significantly increased during quench to result in the large temperature decrease. Finally, the cladding surface rewetted (liquid-surface contact) as the surface temperature dropped below the Lidenfrost temperature. The calculated rewet temperature is about 600 to 650 K for these test conditions. However, no inflection of the data (Figure 7) is noted at this temperature to indicate the exact time of rewet. Therefore, any increases in the surface heat transfer after rewet must not have significantly influenced the rate of cladding temperature decrease that was established during the quench.

As mentioned, the rod internal thermocouples and LVDT measured several gradual oscillations in temperature as the rod cooled during reflood. These oscillations are important in understanding any surface thermocouple effects. Apparently, a slug of steam with entrained liquid (precursory cooling) was expelled toward both ends of the flow shroud as a portion of the cladding quenched during reflood. The inlet turbine measured a negative (or reversed) coolant flow as this steam expanded. After sufficient time for steam expansion, reflood liquid again flowed into the shroud and the quenching process continued. These slugs of steam with entrained liquid were first generated at the lower portion of the rod and then moved past the thermocouples. Therefore, thermocouple effects can be expected during reflood when a slug of steam with entrained liquid moves past a thermocouple location.

Behavior of Rod 02

The thermal and mechanical response during Test TC-1A of Rod 02, a rod with both external and internal cladding thermocouples, is presented in Figures 8 through 10. Selected internal fuel and internal and external cladding thermocouple data are shown, together with the LVDT data. The Rod 02 measurements are presented for the entire test in Figure 8. Blowdown and reflood results are highlighted in Figures 9 and 10, respectively. The internal and external cladding temperatures at the thermocouple locations decreased after initiation of the blowdown transient until CHF occurred at about 3 s. External and internal cladding temperatures rapidly increased following CHF and reached a peak of 970 and 1010 K, respectively, prior to the slug period. The measured fuel surface

temperature was 1060 K prior to the slug event. All temperatures then decreased between 7 and 9 s as the two-phase slug coolant improved the cladding heat transfer. Fuel and cladding temperatures increased after 9 s and were intentionally adjusted after 20 s, by reactor power adjustments, to an average cladding temperature of about 1030 K prior to reflood.

The Rod 02 thermocouples indicated a time-of-CHF of 3 s, which was significantly later than the Rod 01 CHF time. A cracked weld found on the Rod 02 flow shroud may have influenced the time-to-CHF during some of the TC-1 transients. However, this leakage is not considered significant during Test TC-1A. Evidently, the external thermocouples of Rod 02 delayed CHF as compared with the occurrence of CHF on Rod 01. Both internal and external thermocouples responded in a similar fashion during the two-phase slug period. The external thermocouples provided a good measurement of the rod thermal response as the high quality coolant flowed past the thermocouples. The external and internal thermocouples also responded in a similar fashion during reflood. As previously described, the reflood water apparently entered the flow shroud at the inlet and quenched the cladding slowly, then rapidly, sending low quality liquid slugs past the thermocouple junctions early in reflood. All thermocouples measured the expected oscillating temperature trends prior to cladding quench as these low quality slugs passed the surface thermocouples. However, the external thermocouples measured large (~100 K) temperature oscillations prior to quench due to the two-phase slugs. In comparison, the internal thermocouples oscillated by only about 50 K as a result of the same two-phase slugs. The external thermocouples extending into the coolant stream probably measured larger than actual cladding temperature oscillations during reflood.

Behavior of Rod 03

The thermal and mechanical response of Rod 03, a rod with three fuel thermocouples and four external cladding surface thermocouples, is presented in Figures 11 through 13. Data from the entire Test TC-1A are presented in Figure 11 for two of the internal fuel thermocouples, one external cladding thermocouple, and the LVDT (the internal fuel thermocouple of Rod 03 at the 220-degree orientation did not function). Similar

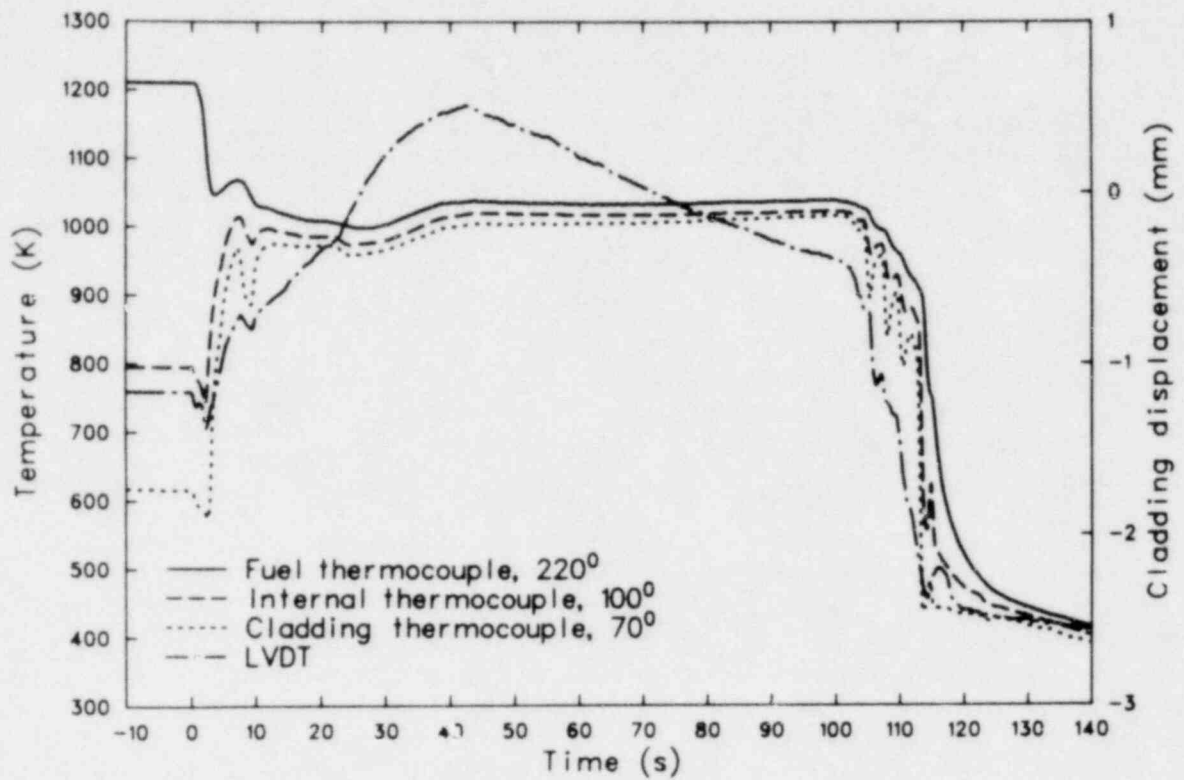


Figure 8. Rod internal and cladding surface temperatures, and cladding axial displacement of Rod 02 during Test TC-1A.

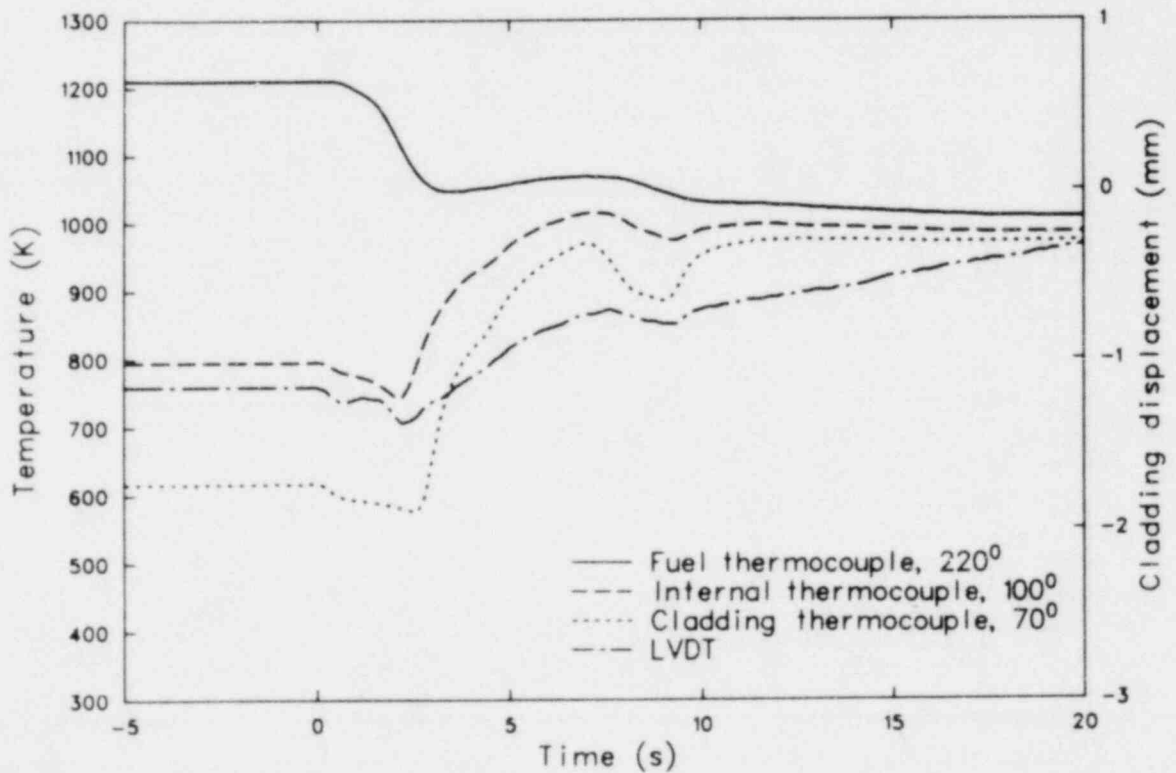


Figure 9. Rod internal and cladding surface temperatures, and cladding axial displacement of Rod 02 during blowdown phase of Test TC-1A.

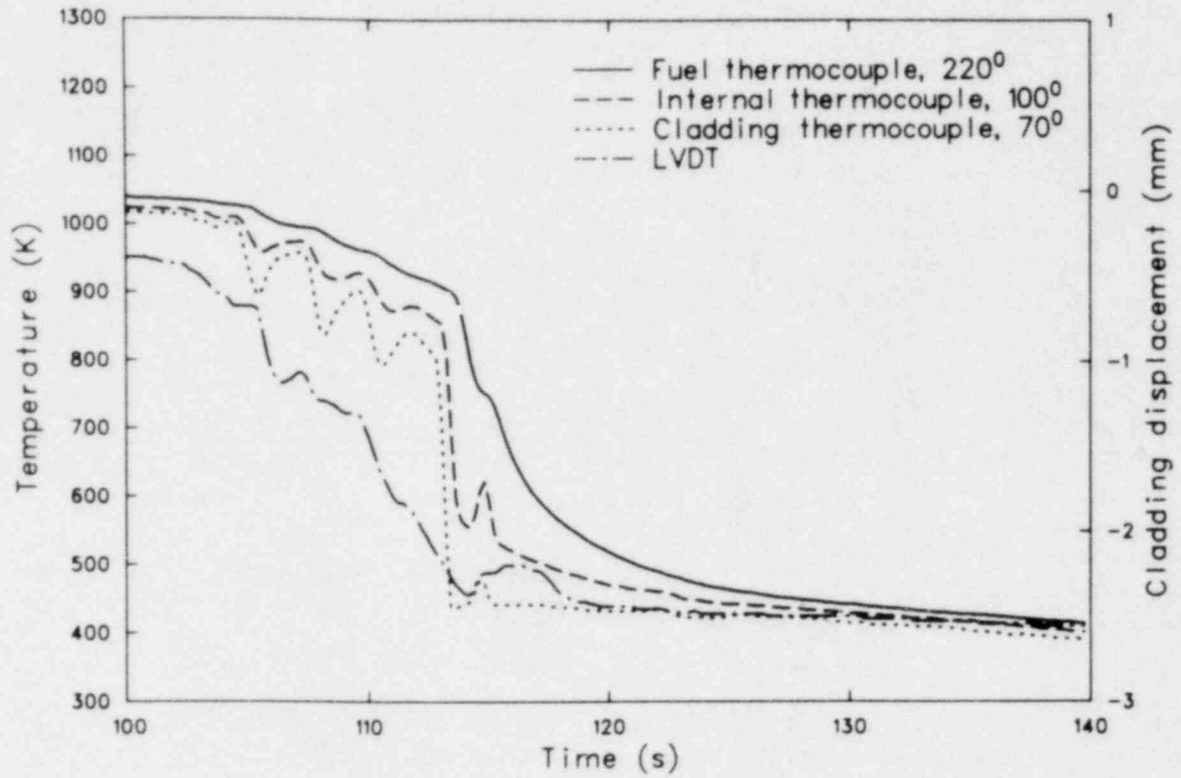


Figure 10. Rod internal and cladding surface temperatures, and cladding axial displacement of Rod 02 during reflood phase of Test TC-1A.

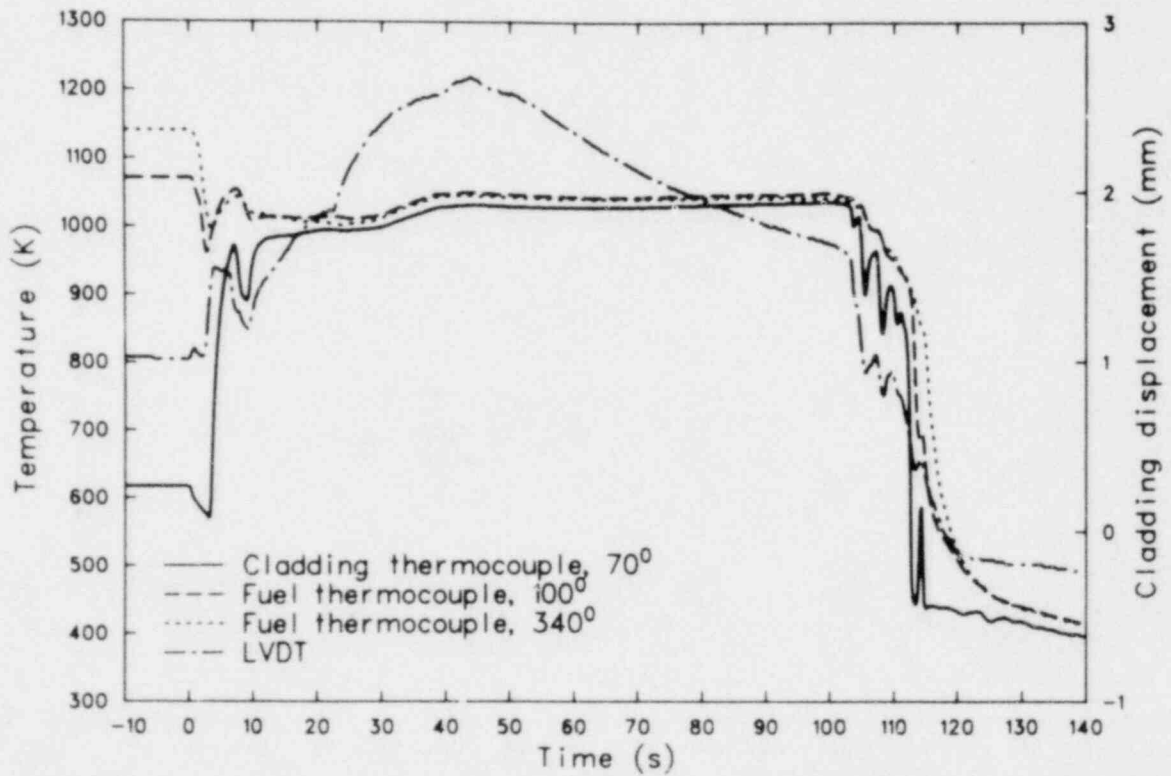


Figure 11. Rod internal and cladding surface temperatures, and cladding axial displacement of Rod 03 during Test TC-1A.

results for the first 20 s of blowdown and the 40 s of reflood are presented in Figures 12 and 13, respectively. The internal and external temperatures gradually decreased until about 2 to 3 s, when CHF occurred. External cladding and internal fuel temperatures rapidly increased following CHF and reached 980 and 1050 K, respectively, before the slug phase began at 7 s. The cladding temperatures gradually decreased during the slug phase as the high quality two-phase coolant passed through the flow shrouds. Following blowdown, fuel and cladding temperatures stabilized at 1040 K and the reflood phase was initiated at about 100 s.

The Rod 03 fuel and cladding temperatures began to decrease at 103 s (3 s into reflood). Measured temperatures first decreased by about 15 K/s and gradually oscillated as the inlet reflood rate oscillated until 112 s. Quench, or a rapid temperature decrease, occurred at 112 s, which was earlier than the quench of Rod 01. As described for Rod 02, the external thermocouples on Rod 03 measured several rapid temperature oscillations in excess of 100 K as the two-phase reflood precursory cooling passed the thermocouple junctions. However, these measured temperature oscillations

are probably larger than the actual cladding temperature oscillations because the external thermocouples protruded into the coolant channel and were therefore preferentially cooled. Results of each TC-1 test support this conclusion and, in fact, when the internal thermocouples did not measure cladding quenches, the external thermocouples sometimes completely quenched to the coolant saturation temperature, followed by thermocouple reheating. The external thermocouples apparently indicated larger than actual cladding temperature decreases as the two-phase liquid precursory cooling passed the thermocouples during reflood, and sometimes acted independently of the cladding by momentarily quenching before the cladding quenched.

Behavior of Rod 04

The thermal and mechanical response during Test TC-1A of Rod 04, a rod with three fuel thermocouples but no cladding thermocouples, is presented in Figures 14 through 16. The internal fuel thermocouple and LVDT measurements during the entire test are presented in Figure 14. Similar responses for the first 20 s of blowdown

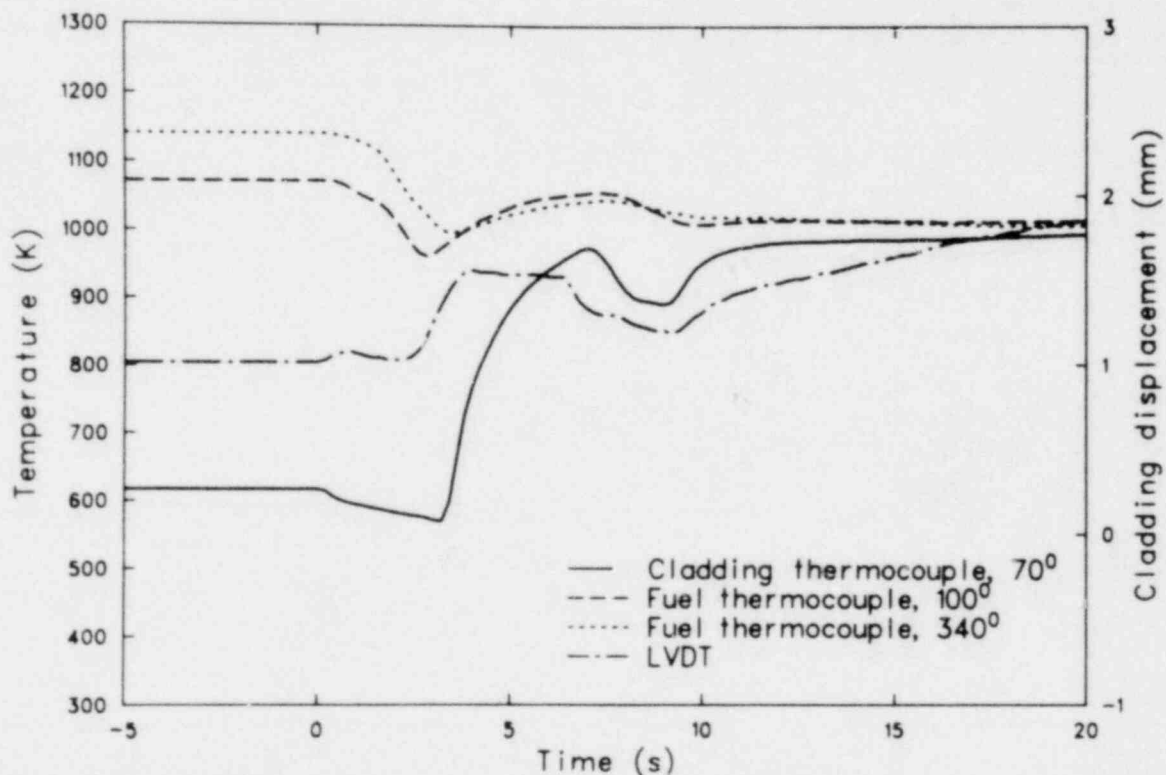


Figure 12. Rod internal and cladding surface temperatures, and cladding axial displacement of Rod 03 during blowdown phase of Test TC-1A.

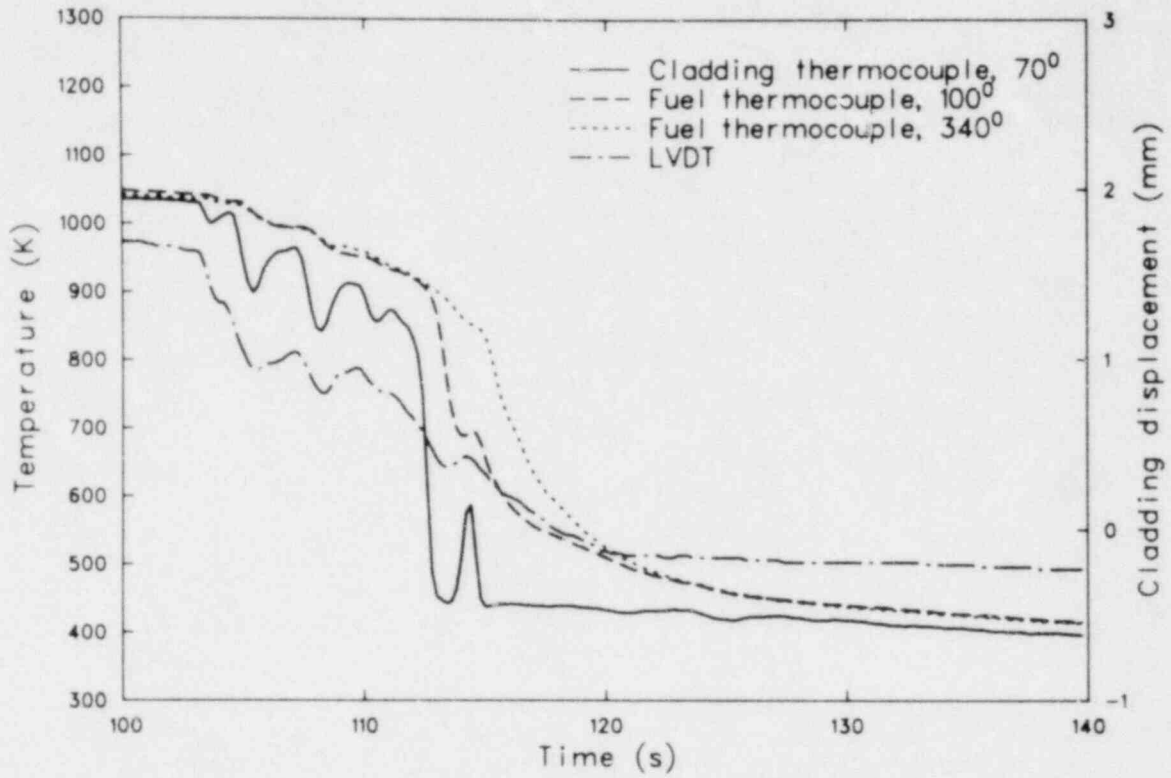


Figure 13. Rod internal and cladding surface temperatures, and cladding axial displacement of Rod 03 during reflood phase of Test TC-1A.

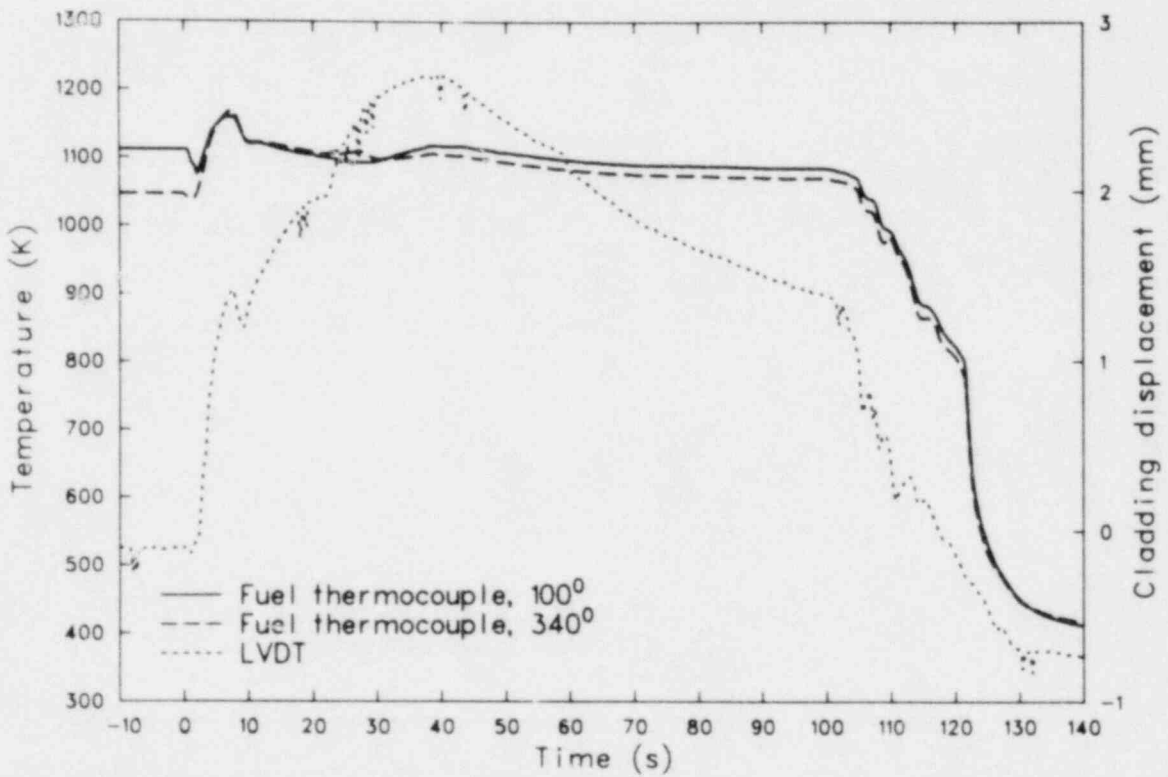


Figure 14. Rod internal temperatures and cladding axial displacement of Rod 04 during Test TC-1A.

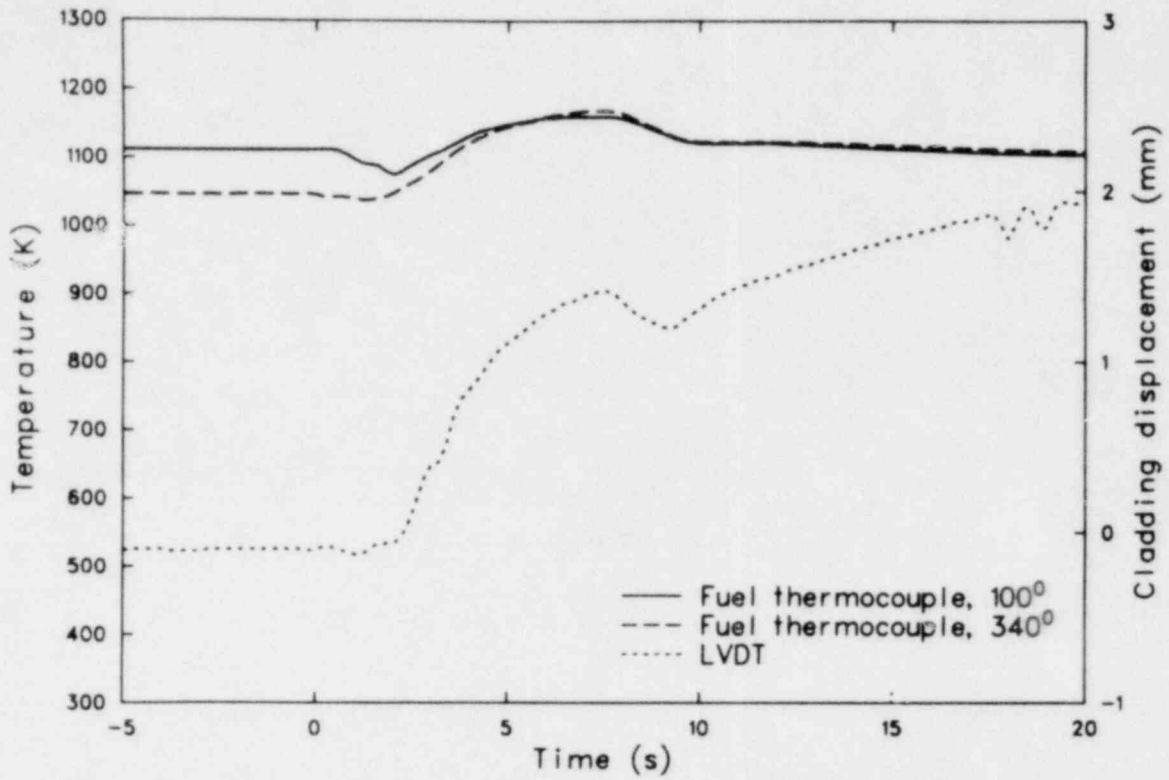


Figure 15. Rod internal temperatures and cladding axial displacement of Rod 04 during blowdown phase of Test TC-1A.

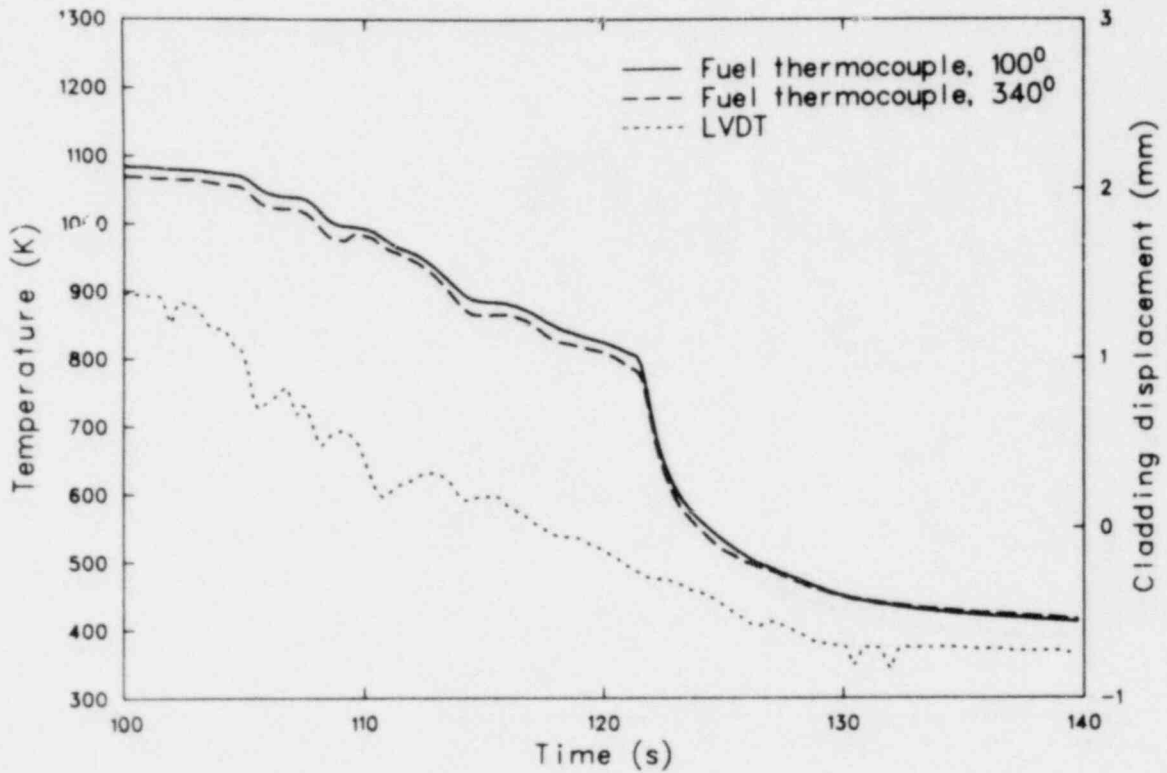


Figure 16. Rod internal temperatures and cladding axial displacement of Rod 04 during reflood phase of Test TC-1A.

and the 40 s of reflood are presented in Figures 15 and 16, respectively. The internal fuel temperatures generally decreased for about 2.0 s until CHF occurred at the thermocouple junctions. The LVDT measured an axial increase in length at about 1 s, indicating an earlier occurrence of CHF at some other location on the fuel rod. Internal fuel peak temperatures reached 1180 K before the

slug phase was initiated. The cladding and fuel temperatures gradually decreased after 7 s until the end of the slug phase. Fuel temperatures stabilized at 1100 K prior to reflood.

The thermal and mechanical behavior of Rod 04 during reflood was similar to the behavior of Rod 01, discussed previously.

COMPARISON OF SELECTED RESULTS

Selected test data from rods with and without cladding surface thermocouples are compared in this section to better illustrate the effects of external thermocouples on the thermal behavior of light water reactor fuel rods during a severe loss-of-coolant accident. The internal fuel rod temperatures during the entire Test TC-1A transient are first compared. The LVDT data from the first 30 s of all four TC-1 blowdown transients are then presented, along with the internal fuel and cladding temperatures of each rod during the first 10 s of Test TC-1A. Finally, the internal fuel and cladding temperature data, from rods with and without cladding surface thermocouples, during the reflood phase of all four TC-1 blowdown transients are compared.

Comparison of Selected Internal Cladding and Fuel Surface Temperatures During Test TC-1A

The internal cladding and fuel surface temperatures of the rods with and without external thermocouples are compared on a one-to-one basis in Figures 17 through 20. The time of CHF at the thermocouple junctions within Rods 01 and 04 (rods without external thermocouples) was approximately 0.9 and 2.0 s, respectively, compared with about 3 s for the two rods with external thermocouples. The fuel stored energy rapidly decreased during the time prior to CHF, since the initial heat transfer mechanism was nucleate boiling. Therefore, the measured temperatures within Rods 02 and 03, the rods with external thermocouples, were about 100 to 150 K lower than the temperatures of Rods 01 and 04 throughout blowdown. The temperatures within all four TC-1 test rods prior to reflood converged to within about 1050 to 1100 K. The cladding cooling trends during reflood were similar for each rod; however, the rods with external thermocouples quenched (experienced a rapid temperature decrease) before the rods without external surface thermocouples.

Comparison of LVDT and Internal Temperature Results During Blowdown

Cladding axial extensions during blowdown are compared in Figures 21 through 24. (As men-

tioned above, the Rod 01 LVDT electronics did not function properly during Tests TC-1A and TC-1B.) The LVDTs measured the length of the fuel rod cladding; however, the base of the instrument was also attached to the test train flow shroud; hence, variations in the flow shroud dimensions also influenced the measurement. The data shown in Figures 21 through 24 were corrected to eliminate effects associated with shroud length changes by estimating the shroud temperature, based on results of other PBF LOCA tests,⁷ and then calculating and subtracting shroud length variations from the cladding length changes.

The LVDT measurements provide a good indication of total fuel rod heating and cooling trends. The results are, however, sometimes difficult to interpret if the fuel rod heating trends are not consistent along the entire length of the rod. For example, CHF may not occur uniformly along the length of a fuel rod during a LOCA; rather, a portion of the cladding may have experienced CHF and may be heating and expanding while the remainder of the cladding is cooling and contracting prior to CHF. The total rod elongation might then indicate no (or only a small relative) change in the average cladding length. The exact time of CHF would then be difficult to determine on the basis of LVDT measurements.

The measured CHF times, based on the LVDT responses during the different transients, are summarized in Table 1. The cladding of Rods 01 and 04, which did not have external surface thermocouples, generally began expanding due to rapid heating after CHF between 0.8 and 1.5 s after initiation of the transient. In comparison, the time of CHF on Rods 02 and 03, rods with external thermocouples, was between 2.4 and 2.5 s. The determination of the exact time of CHF on Rods 01 and 03 during all of the TC-1 transients is straightforward, and the Rod 01 CHF consistently occurred well before the Rod 03 CHF. The exact time of CHF on Rod 04 is more difficult to determine. The Rod 04 LVDT measurement was noisy, with small negative spikes occurring at various times during each test. These negative spikes are not considered an accurate measurement of rod elongation, but rather a result of electronic noise in the data system. Unfortunately, a noise spike occurred near the time of

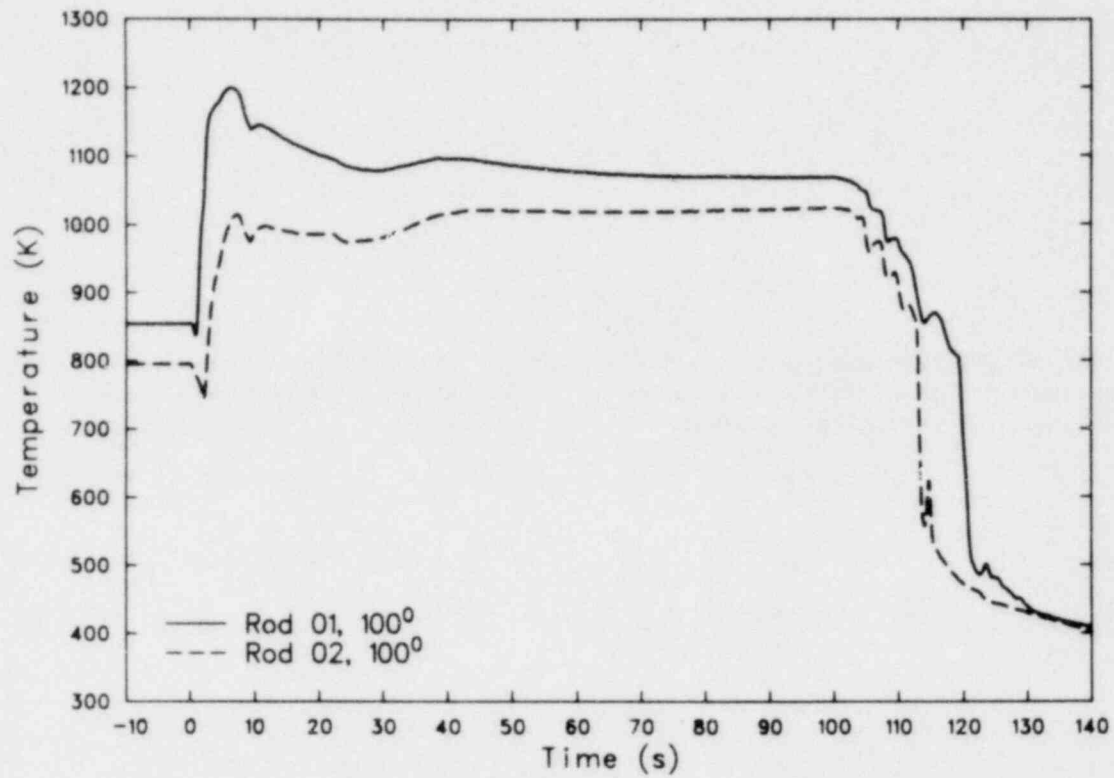


Figure 17. Comparison of internal cladding temperatures of Rods 01 and 02 during Test TC-1A.

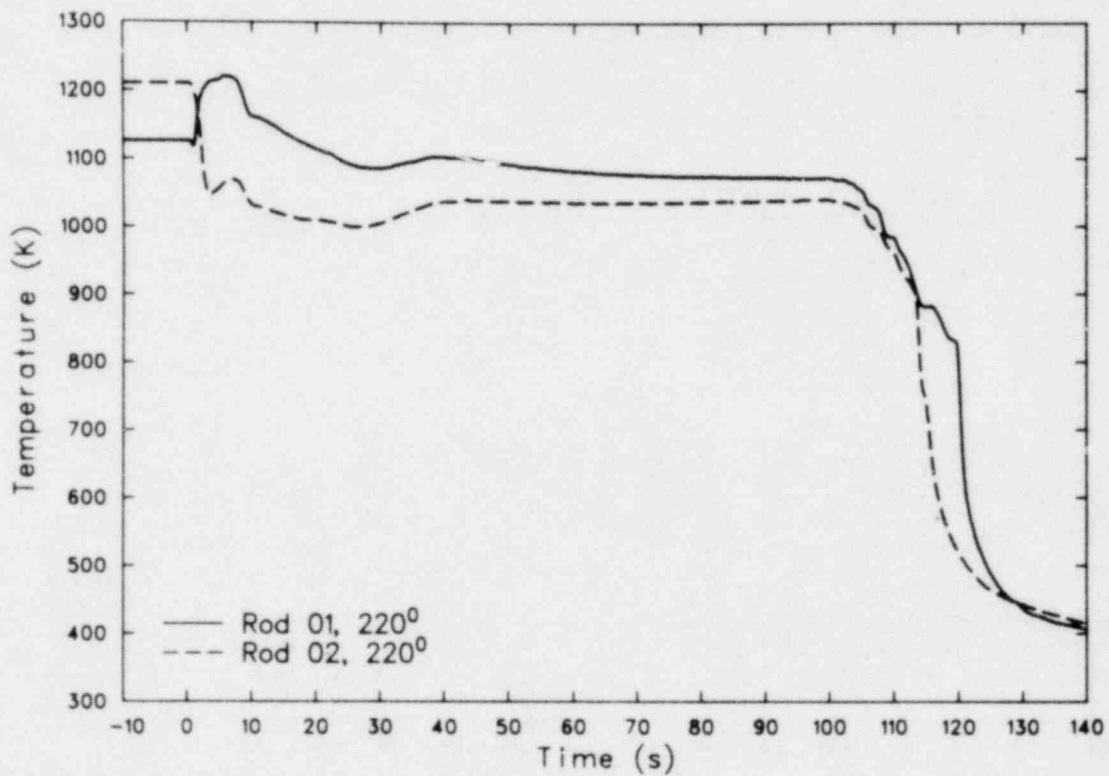


Figure 18. Comparison of internal fuel temperatures of Rods 01 and 02 during Test TC-1A.

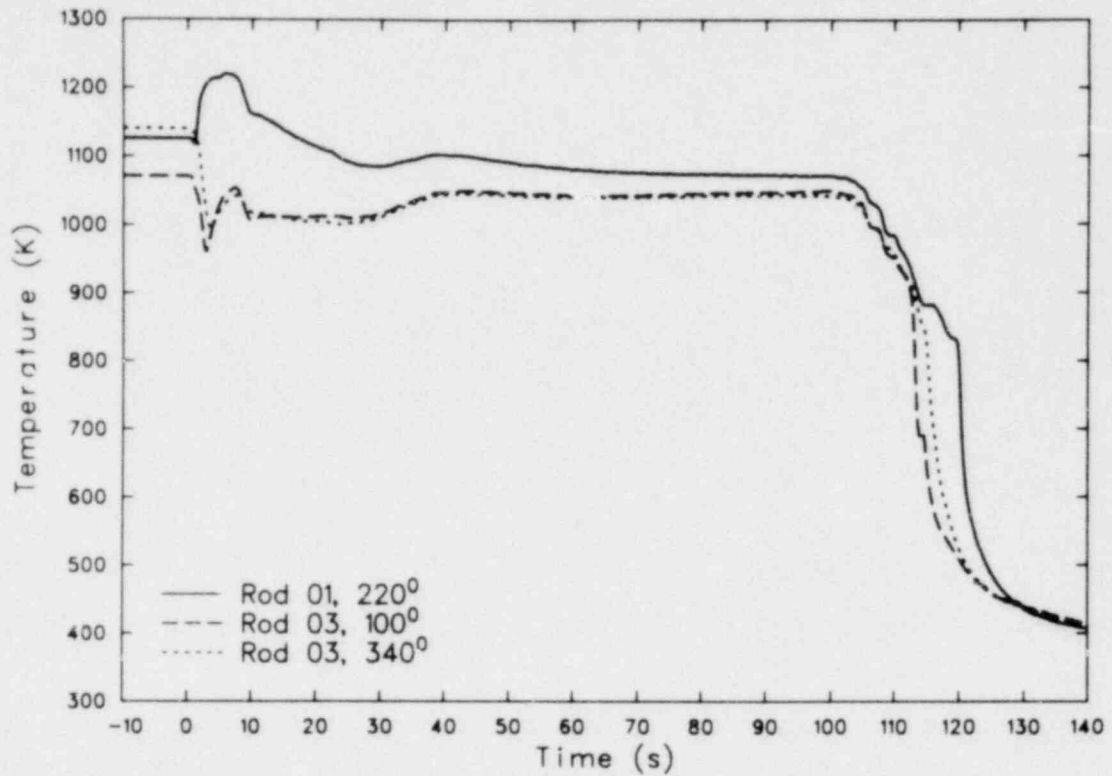


Figure 19. Comparison of internal fuel temperatures of Rods 01 and 03 during Test TC-1A.

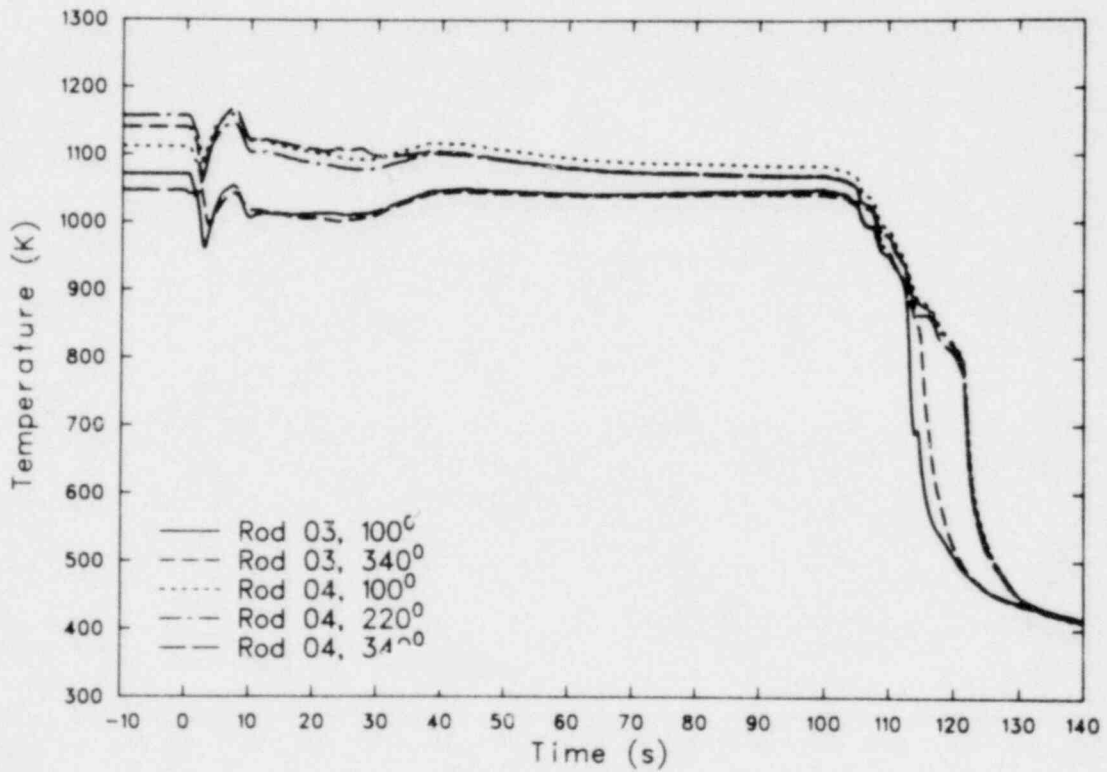


Figure 20. Comparison of internal fuel temperatures of Rods 03 and 04 during Test TC-1A.

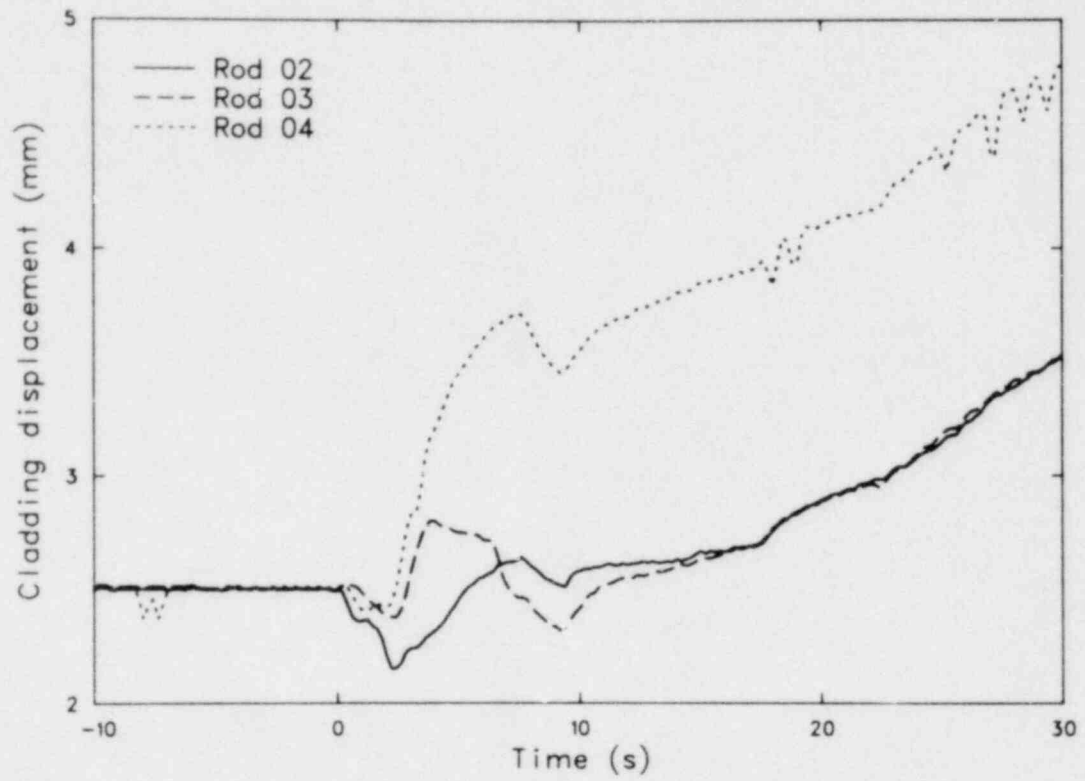


Figure 21. Comparison of cladding axial displacement measurements during Test TC-1A.

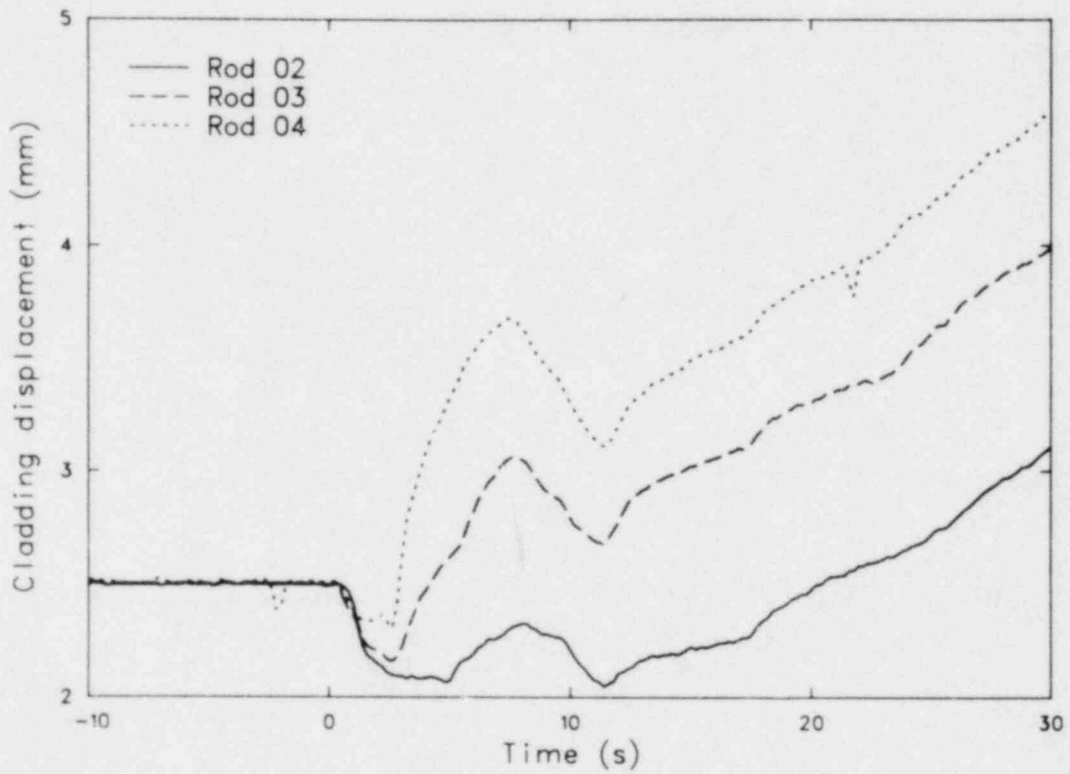


Figure 22. Comparison of cladding axial displacement measurements during Test TC-1B.

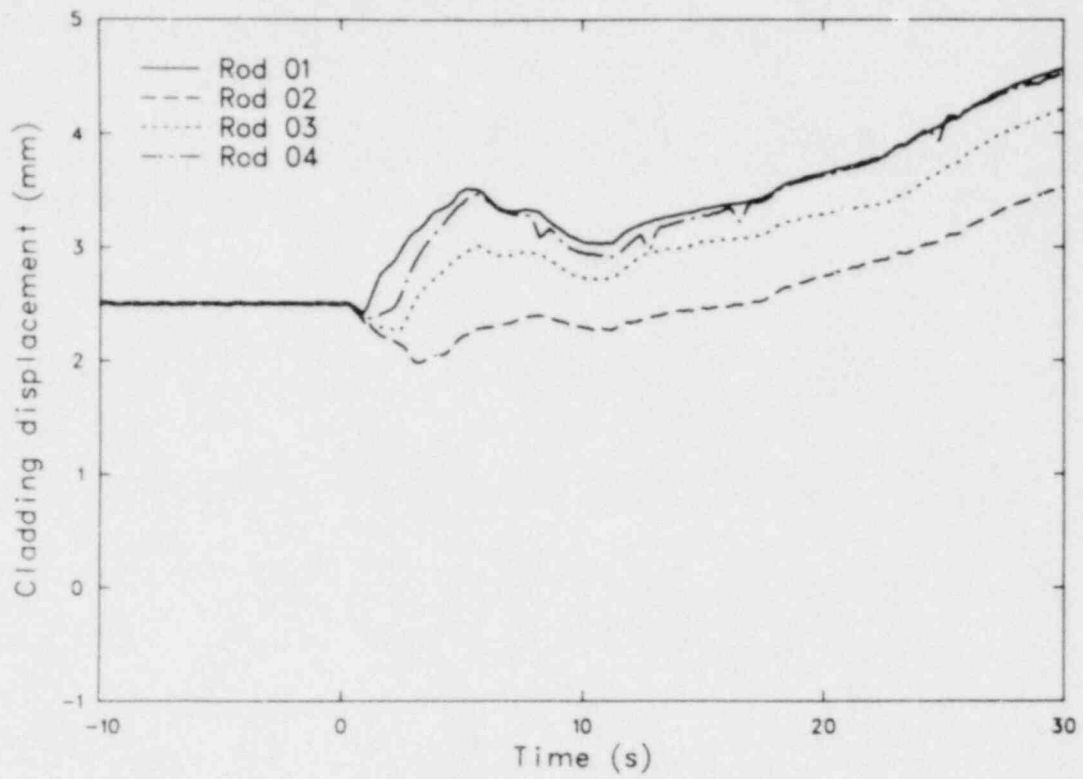


Figure 23. Comparison of cladding axial displacement measurements during Test TC-1C.

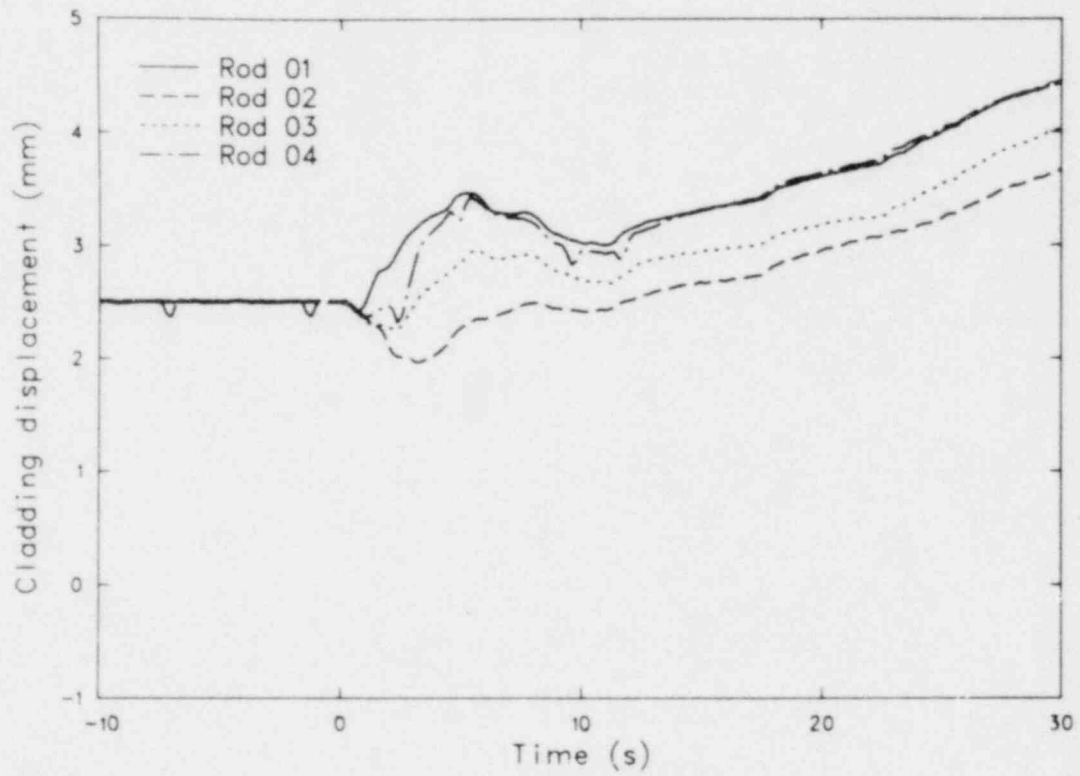


Figure 24. Comparison of cladding axial displacement measurements during Test TC-1D.

Table 1. Comparison of CHF times^a for all TC-1 rods

<u>Test</u>	<u>Rod 01</u>	<u>Rod 02</u>	<u>Rod 03</u>	<u>Rod 04</u>
TC-1A	b	2.4	2.4	1.2
TC-1B	b	c	2.5	1.5
TC-1C	0.9	c	2.5	1.2
TC-1D	0.8	c	2.5	1.1

a. Times based on the LVDT response in seconds.

b. LVDT did not function.

c. Rod 02 shroud leakage occurred.

CHF during almost all of the TC-1 transients, making the exact time of CHF difficult to determine. However, the Rod 04 time of CHF was always at least 1 s before the Rod 03 CHF. Therefore, on the basis of the TC-1 cladding elongation measurements, external cladding thermocouples delay the time of CHF.

The internal fuel rod temperature responses during the first 10 s of Test TC-1A are presented in Figures 25 through 28. These data were also used to determine the CHF time within each rod. Rods 01 and 04, without surface thermocouples, should have had similar times-to-CHF and comparable temperatures since the rods were similar. However, a review of the temperatures presented in Figures 25 and 28 shows a significant difference in the time of CHF between these rods. Critical heat flux consistently occurred at about 1 s on Rod 01, which corresponded well with the LVDT response. The Rod 04 CHF consistently occurred at about 2 to 2.5 s at the thermocouple junctions. The axial elongation measurements presented earlier indicate that the Rod 04 CHF apparently occurred at about the same time as the Rod 01 CHF and at about the same location on the rod. The leakages found at the centering screws or at the upper turbine on the shroud of Rod 04 possibly influenced the time of CHF or enhanced momentary rewets at the thermocouple junctions. The cladding axial extension of Rods 01 and 04 consistently converged to the same value at about 15 s after initiation of blowdown. Since the reactor power was maintained at a low level throughout blowdown, the cladding temperature

of both rods should eventually converge as the Rod 04 shroud leakage decreased late in the blowdown.

The peak temperatures of each TC-1 transient measured by all internal fuel thermocouples are compared with the CHF times in Figure 29. Four data points, one for each test, are presented for each rod, except Rod 02 for which only Test TC-1A results are presented. In the case of Rods 03 and 04, in which more than one internal fuel temperature was measured at the junction elevation, the data represent an average of the available thermocouples. The data were also corrected to account for differences in stored energy between each test resulting from cladding collapse or fuel relocation.

A CHF time of about 1 s at the thermocouple junctions of Rod 01 resulted in a fuel peak temperature of about 1225 K. In comparison, a 2.4-s CHF time resulted in a Rod 04 peak temperature of about 1160 K. It should be noted that the Rod 04 CHF time applies to the thermocouple junctions only, since the LVDT-measured CHF times (provided in Table 1) indicated that CHF on Rods 01 and 04 probably occurred at similar times over most of the axial length. However, since a significant difference in CHF times did occur at the thermocouple junctions of Rods 01 and 04, a comparison of temperatures reached during blowdown is possible between these rods and demonstrates the influence of CHF time on blowdown temperatures for rods without external thermocouples. A line was fit through the data

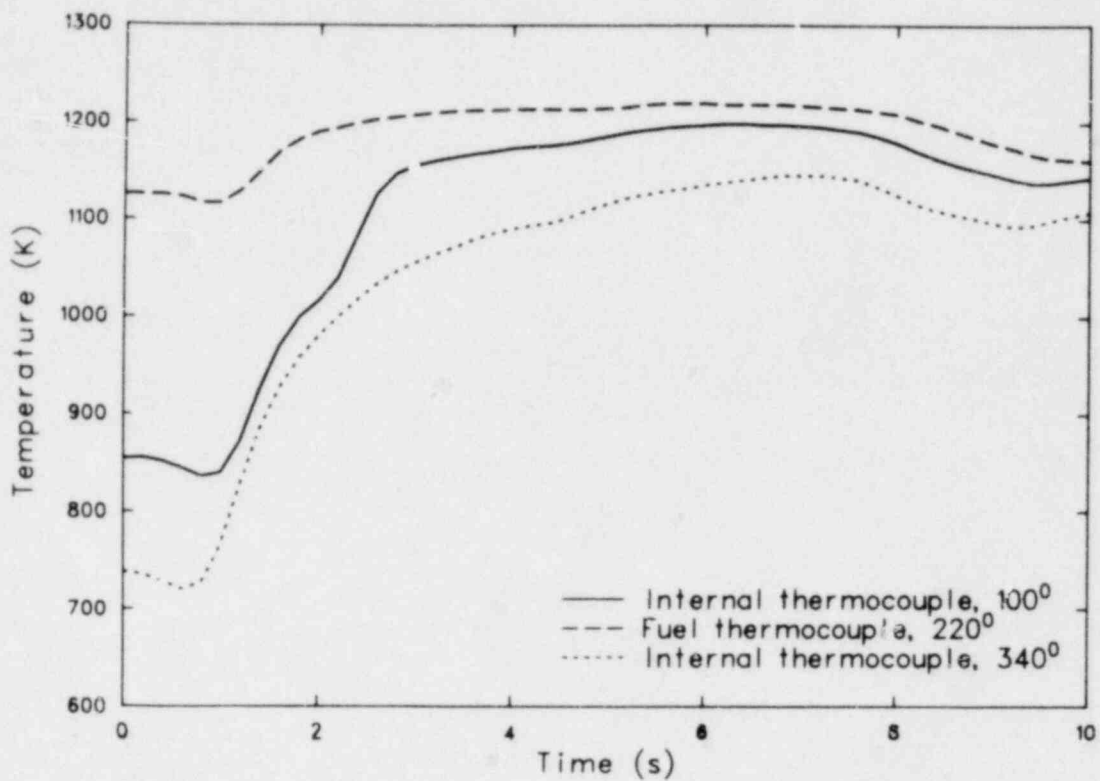


Figure 25. Comparison of internal fuel and cladding temperatures of Rod 01 during Test TC-1A.

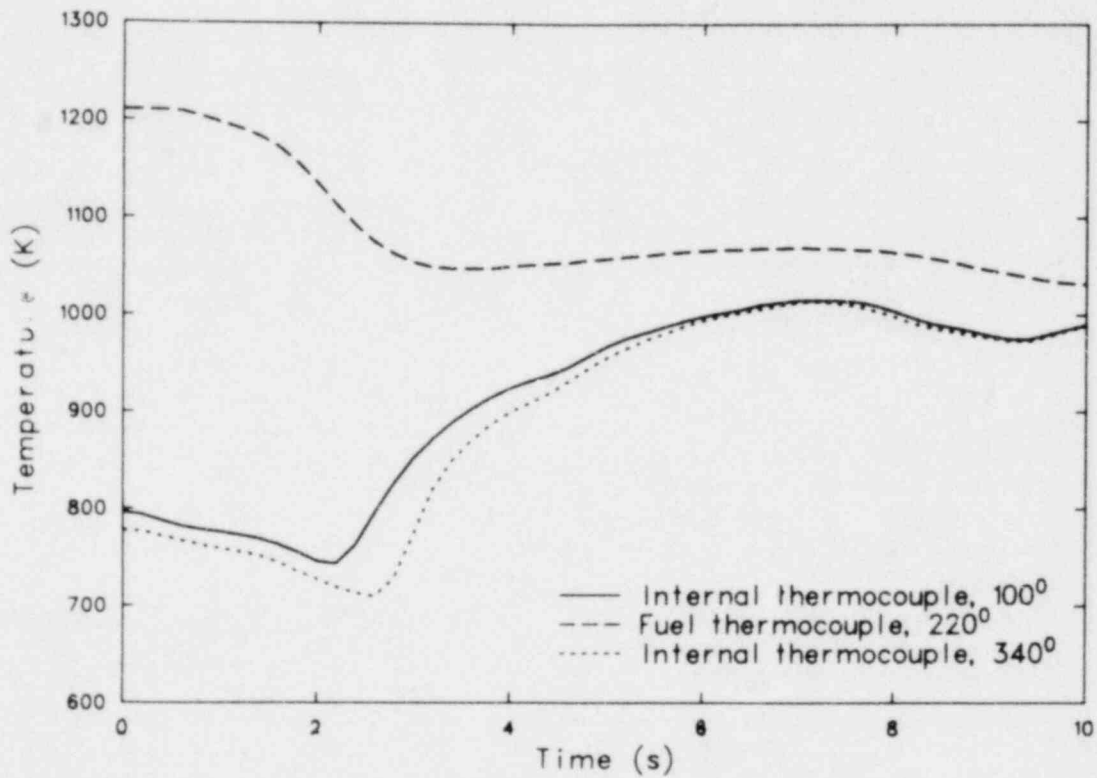


Figure 26. Comparison of internal fuel and cladding temperatures of Rod 02 during Test TC-1A.

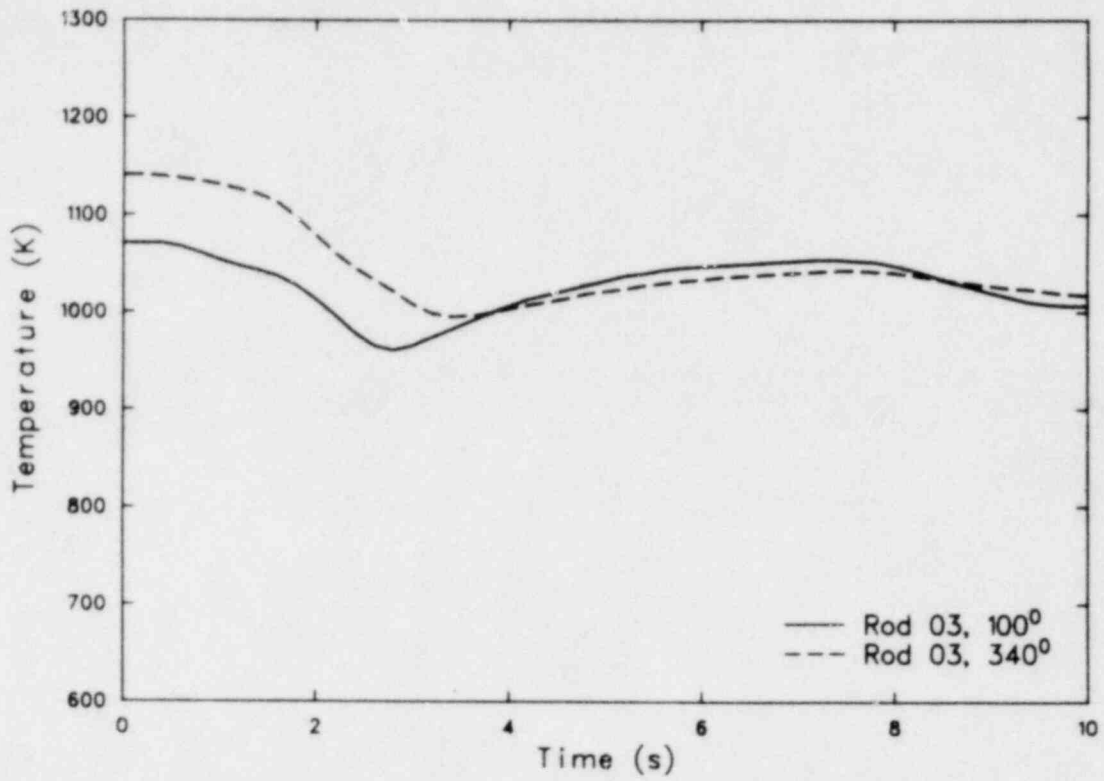


Figure 27. Comparison of Rod 03 internal fuel temperatures during Test TC-1A.

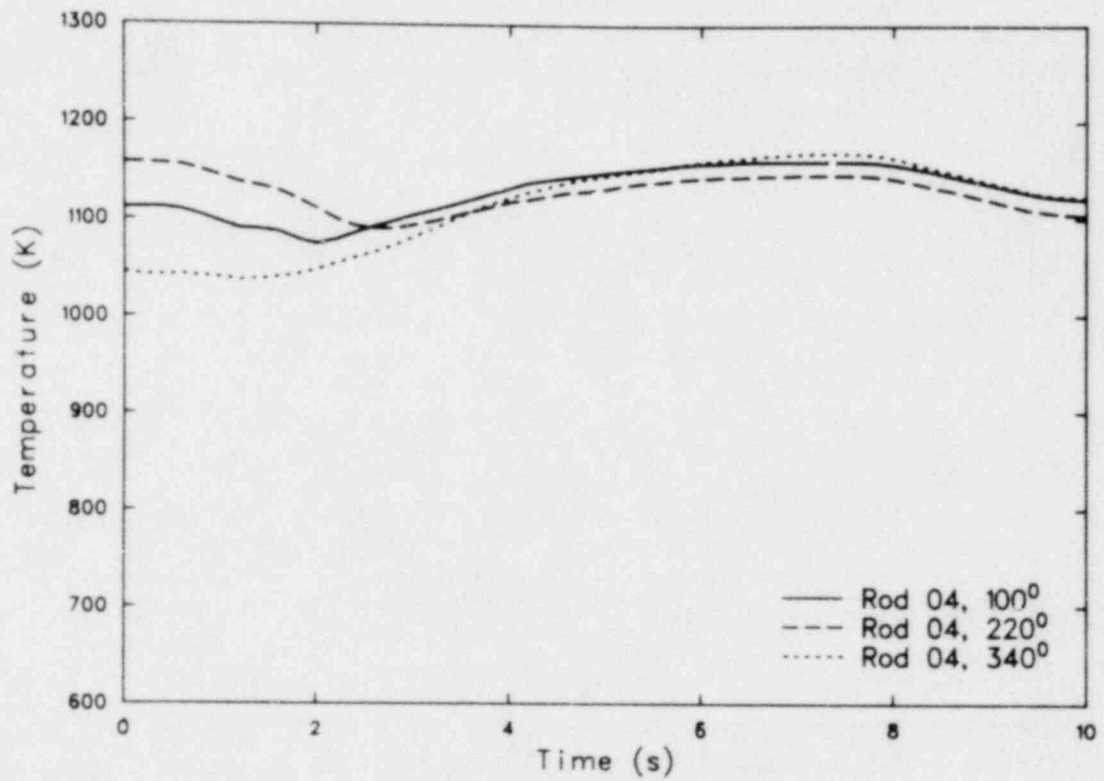


Figure 28. Comparison of Rod 04 internal fuel temperatures during Test TC-1A.

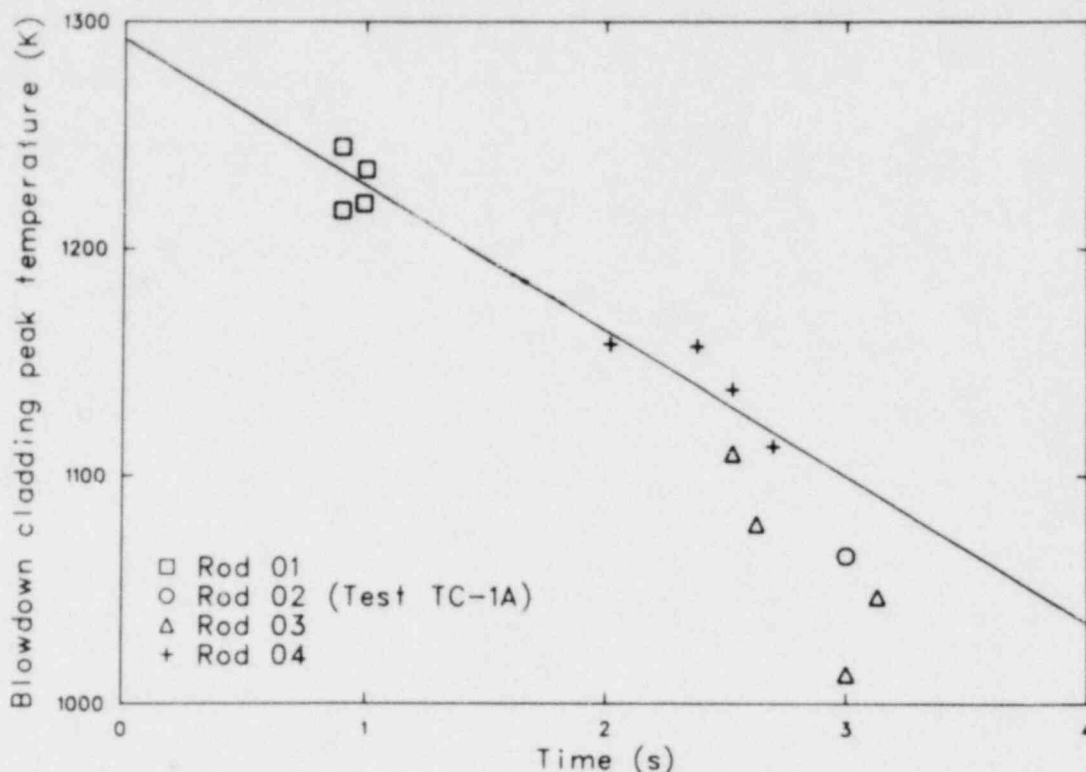


Figure 29. Comparison of blowdown cladding peak temperatures with time-to-CHF during TC-1 tests.

from Rods 01 and 04 (Figure 29) and, generally, each second of delay in CHF was found to result in a 66.1 K decrease in cladding peak temperature during blowdown. The one-sigma uncertainty in the data was calculated to be 11.3 K.

The internal peak temperatures during blowdown for Rods 02 and 03, rods with external thermocouples, were, on the average, about 50 K less than expected from the Rods 01 and 04 curve fits. The lower temperature is probably a result of fin cooling, which enhanced the cladding surface heat transfer during blowdown. Therefore, the external cladding thermocouples increased the time of CHF and improved the cladding surface heat transfer, and both mechanisms reduced the cladding temperatures. The data fit shown in Figure 29 is based on limited data, and data from a future test series (TC-3) will be fit to this curve to substantiate these conclusions.

The mechanism for the delay of CHF due to the cladding surface thermocouples can only be speculated. A number of CHF correlations have been developed for use in LOCA analyses. These correlations are typically based on fluid properties that relate CHF to coolant conditions, flow rate, and quality or void fraction. The correlations do

not, however, account for surface conditions or effects associated with geometry distortions due to instruments such as surface thermocouples.

The coolant in the flow shrouds of the PBF LOCA experiments was rapidly expelled from the shroud inlet during the first seconds of blowdown. Prior to CHF, the fuel rods were cooled by coolant moving downward along the cladding. This coolant was subcooled during the first 0.1 s of the blowdown. As the system pressure decreased toward saturation, the coolant began to flash and the fuel rods were efficiently cooled by nucleate boiling heat transfer. The flashing of liquid to steam continued as the liquid inventory within the flow shroud rapidly decreased over the first few seconds of blowdown. Critical heat flux was eventually exceeded and the fuel rod was then blanketed by a vapor film. Fuel rods without surface thermocouples reached CHF within 1.5 s. In comparison, CHF occurred at about 2.5 s on fuel rods with surface thermocouples. The thermocouples were spot welded at 2.54-cm intervals along the length of the cladding surface, and the configuration may have delayed the formation of a vapor film blanket or momentarily trapped liquid on the surface of the rods. The vapor film

formed only after the coolant quality had sufficiently increased. Additionally, the surface thermocouples possibly provided efficient fin cooling for the cladding. The TC-1 results indicate that CHF correlations should account for unusual surface conditions such as thermocouples.

The reduction in cladding peak temperatures due to delayed CHF in the TC-1 tests is consistent with the LOFT Blowdown CHF Test⁵ results. The LOFT out-of-pile CHF tests compared the behavior of two electrically heated 25-rod bundles, one with and one without surface thermocouples. These tests were conducted in hot and cold leg break LOCA environments in which the coolant stagnated early in blowdown and CHF rapidly occurred. The maximum difference in time-to-CHF between bundles with and without surface thermocouples was less than 0.45 s, with most differences less than 0.20 s. An analysis of the behavior of a hot fuel rod during the LOFT L2-4 experiment indicated that a 1-s time difference in CHF could result in a 52-K difference in cladding peak temperature. In comparison, the PBF TC-1 results shown in Figure 29 indicate a 60.1-K difference in cladding peak temperature for each second of delay in CHF.

Comparison of Selected Results During Reflood

A comparison of all TC-1 internal rod thermocouple responses during reflood is provided for each transient in Figures 30 through 33. The comparisons in these figures provide a general summary of all thermocouple results without labeling the location of each thermocouple. On the basis of

these data, fuel rods with external thermocouples consistently quenched 3 to 12 s before the rods without surface thermocouples, with an average difference in quench time of 7.5 s. Additionally, rod quench times were slightly different between each test. Thermocouple quench times of Rods 02 and 03, which were instrumented with surface thermocouples, in Test TC-1C were between 108 and 112 s. Rods 01 and 04, without surface thermocouples, quenched shortly afterwards, between 115 and 118 s. In the repeat test, Test TC-1D, Rods 02 and 03 quenched at about the same times as in Test TC-1C; however, Rods 01 and 04 quenched somewhat later at 120 s. Since the conditions of both tests were essentially the same, the differences in quench times highlight the value of repeat tests, which provide sufficient data to statistically verify the results.

Two mechanisms are identified for early cladding quench of fuel rods with external thermocouples. One, the thermocouple acts as a cooling fin, which quenches early, and then quenches the cladding. This behavior has been reported in out-of-pile experiments. Secondly, the TC-1 rods without surface thermocouples were generally at higher temperatures than the other rods as reflood was initiated. As a result of the higher temperatures, the cladding quench can be expected to take longer. The comparison of rod temperatures provided in Figures 30 through 33 demonstrates that the rods without surface thermocouples experienced about 50 K higher temperatures at the thermocouple location prior to reflood. Both mechanisms will contribute to the resultant quench behavior observed during the TC-1 tests.

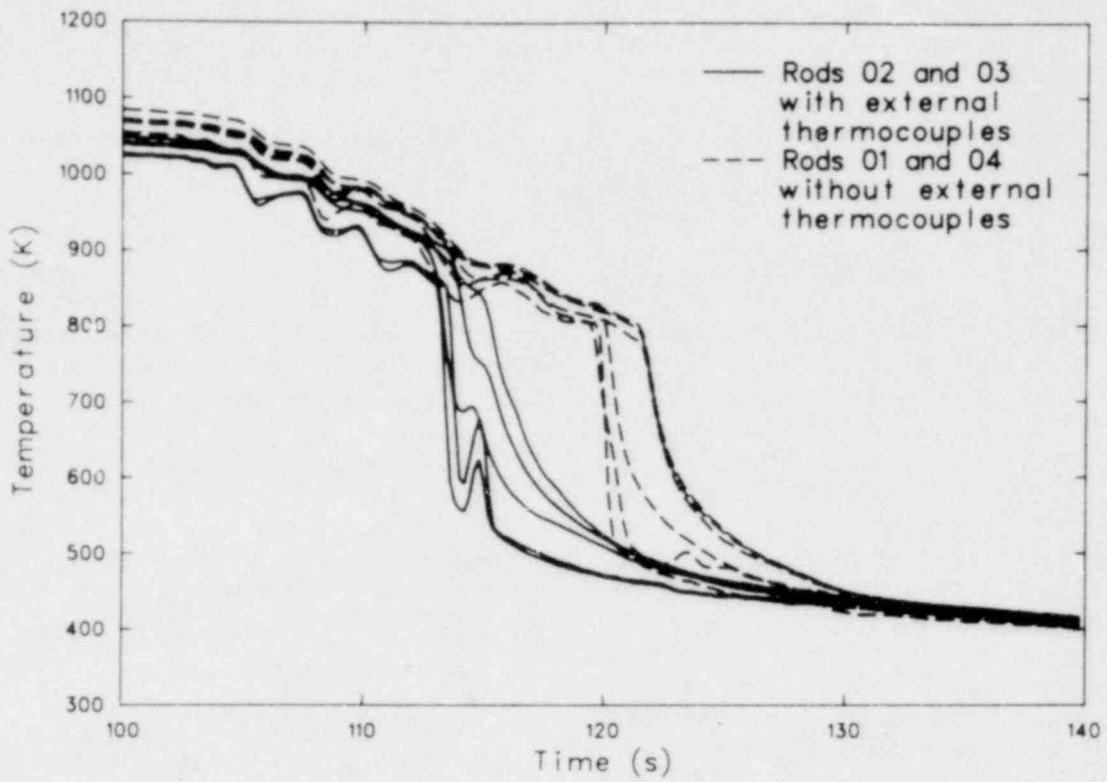


Figure 30. Comparison of all internal rod temperatures during reflood phase of Test TC-1A.

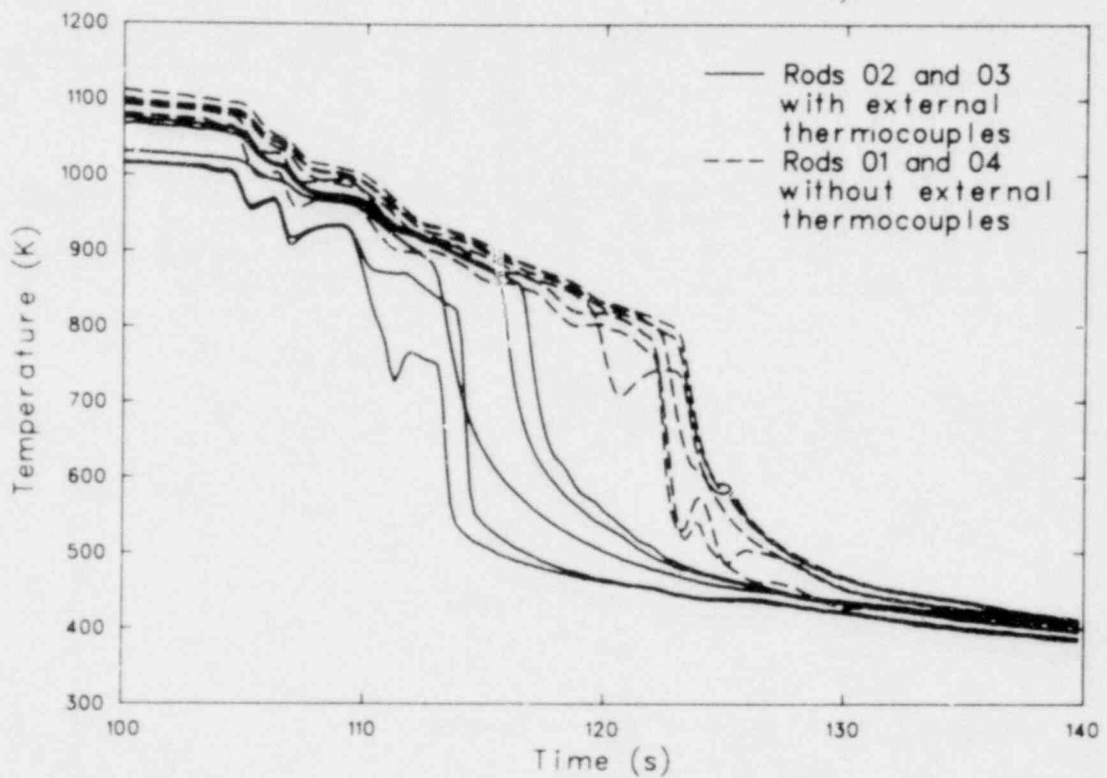


Figure 31. Comparison of all internal rod temperatures during reflood phase of Test TC-1B.

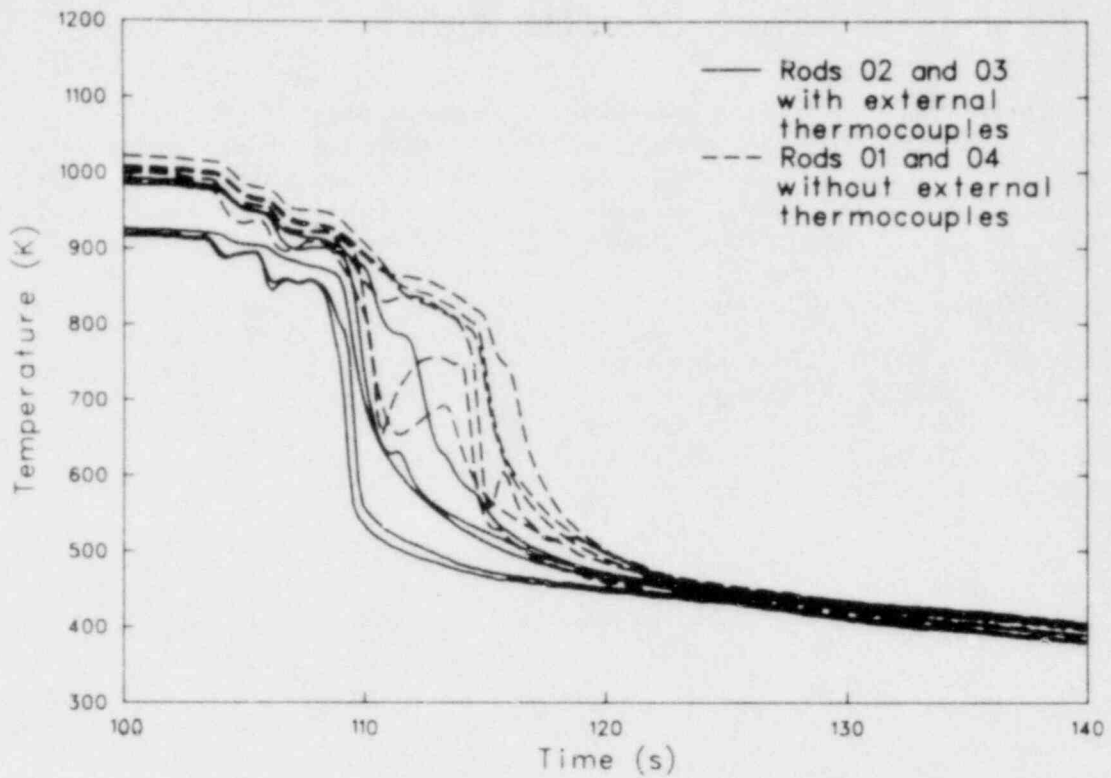


Figure 32. Comparison of all internal rod temperatures during reflood phase of Test TC-1C.

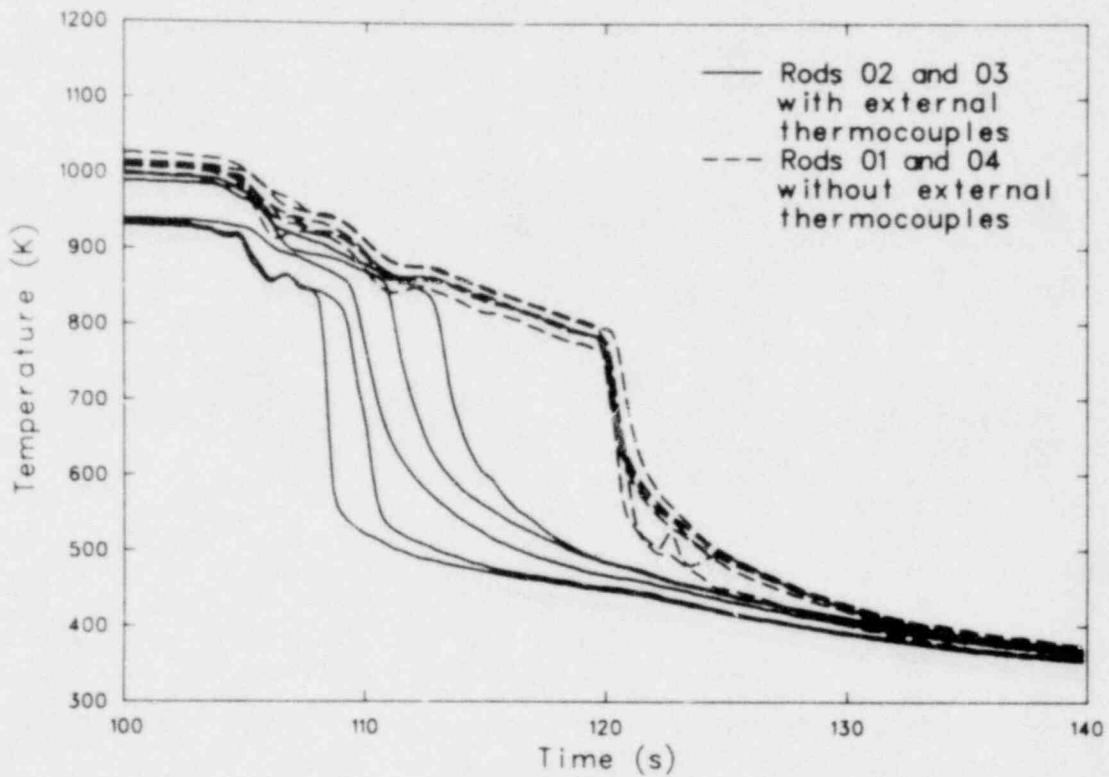
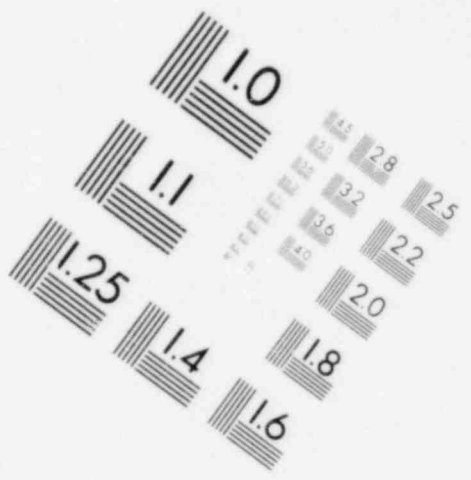
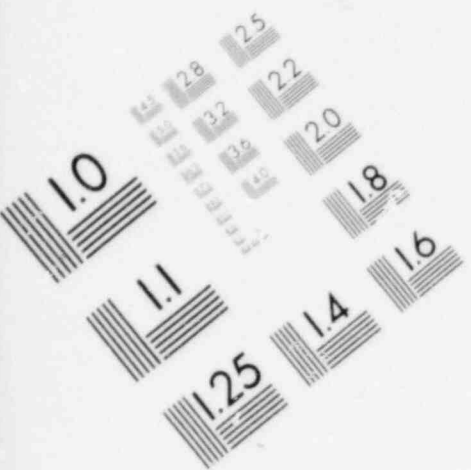
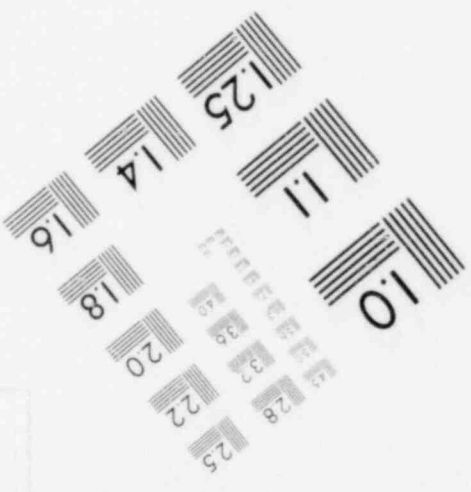
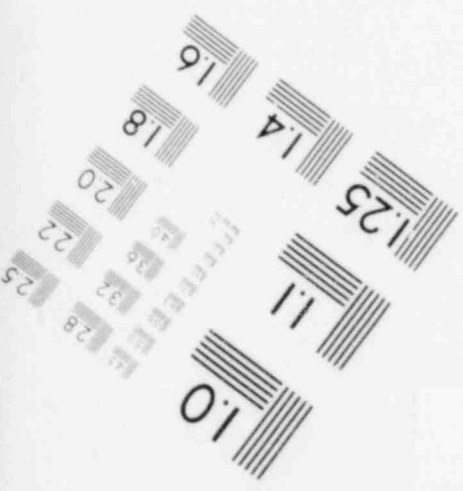
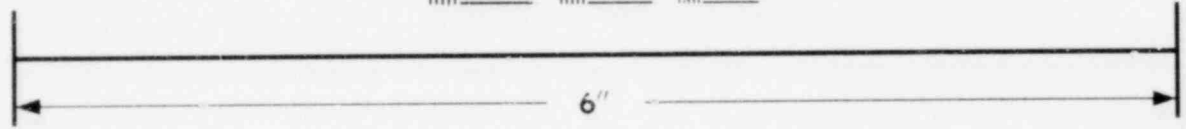
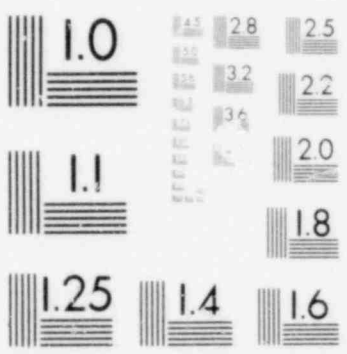
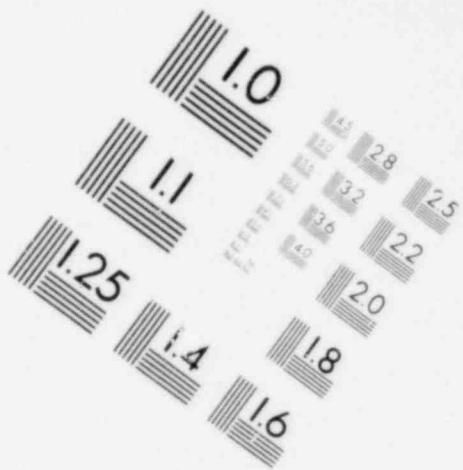
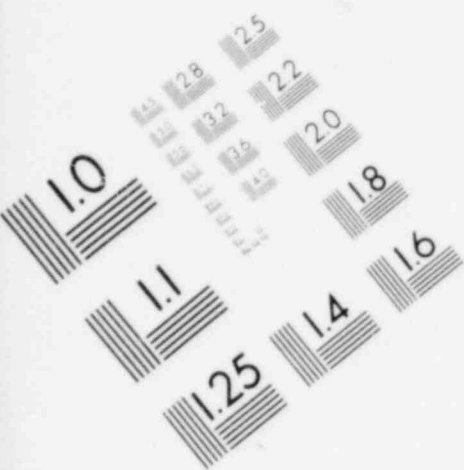


Figure 33. Comparison of all internal rod temperatures during reflood phase of Test TC-1D.

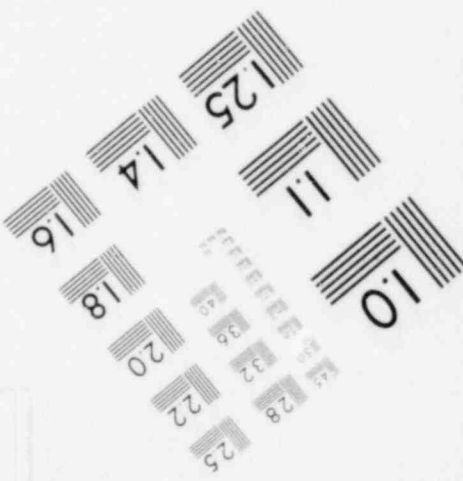
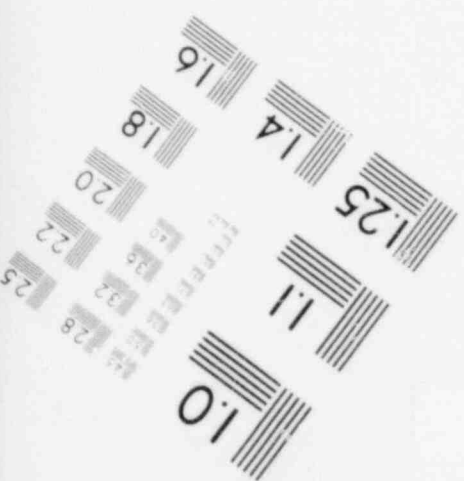
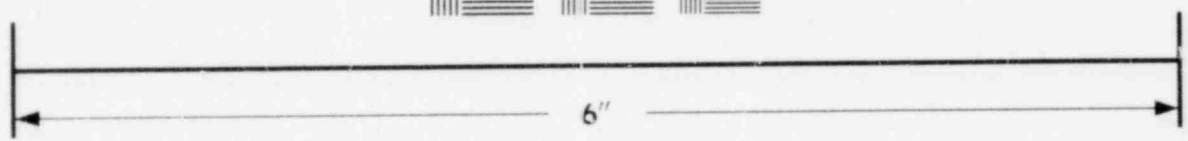
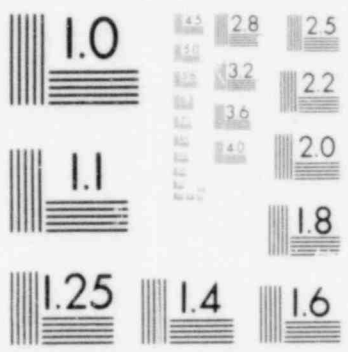


**IMAGE EVALUATION
TEST TARGET (MT-3)**





**IMAGE EVALUATION
TEST TARGET (MT-3)**



CONCLUSIONS

The purpose of the TC-1 tests was to investigate the effects of external cladding thermocouples on the behavior of PWR-type fuel rods during a loss-of-coolant accident. The test provided fundamental insight into the influence of external cladding thermocouples at conditions designed to simulate the LOFT L2-2 and L2-3 experiments.

On the basis of the TC-1 results, we have concluded that surface thermocouples do influence the fuel rod thermal response during both the blowdown and reflood phases of a LOCA. During the blowdown phase, it has been shown that external thermocouples can delay the time-to-CHF and improve the cladding surface heat transfer. The peak temperatures achieved during blowdown were about 60 K lower for each second of delay in CHF. An additional reduction in peak temperatures of about 50 K was measured, apparently a result of enhanced cladding heat transfer due to the external thermocouples.

The surface thermocouples also abetted the cladding quench behavior during reflood. The reflood phase was characterized by (a) cladding temperature turnaround, during which the temperature gradually decreased as steam with entrained liquid passed the thermocouples; (b) quench, during which cladding temperatures rapidly decreased as the quench front passed the thermocouple junction; and (c) rewet, with liquid contacting the cladding surface. For the 4-cm/s reflood rate of the TC-1 tests, no significant difference in the turnaround cladding temperature or initial cooling rate was measured when comparing the response of the rods with and without external thermocouples. However, fuel rods with surface thermocouples quenched and rewetted between 3 and 12 s earlier than the other rods. Additionally, some external thermocouples responded by momentarily quenching and reheating during reflood prior to the actual rod quench. The momentary quenching may have been due to slugs of steam with entrained liquid passing the external thermocouple junctions during reflood.

An attempt was made in the TC-1 tests to simulate the LOFT L2 conditions by forcing a two-phase coolant slug past the fuel rods early in blowdown. Understanding the influence of external thermocouples during the LOFT L2 blowdown, and subsequent rewet, is important in interpreting LOFT results. Generally, all TC-1

thermocouples measured rod cooling during the slug period, but the cladding did not quench as measured during the LOFT L2 experiments. There were no significant differences in the behavior of the TC-1 rods with or without surface thermocouples during this slug period. The TC-1 two-phase slug is believed to have consisted of high quality vapor that could not rapidly quench the rods. To properly simulate LOFT conditions, the liquid content of the two-phase slug should be increased. A means of attaining these conditions in the PBF has been identified and a second test series, designated TC-3, is planned to investigate thermocouple effects during a low quality blowdown quench.

Interpretation of the LOFT data and similar programs (in which external thermocouples are employed) should be viewed in light of the TC-1 results. The thermocouples used in the LOFT experiments measured CHF within 1 to 1.6 s. If CHF occurred on rods without cladding surface thermocouples between 0.5 and 1.0 s earlier, the cladding peak temperatures of those rods during blowdown may have been 30 to 60 K higher. The cladding thermocouples may also have enhanced the surface heat transfer characteristics after CHF, thus reducing the rod peak temperature. Assuming the TC-1 results are directly applicable, the LOFT rods without cladding thermocouples may actually have been an additional 50 K hotter than the rods with external thermocouples, which reached CHF at the same time. The total difference in cladding peak temperature between the LOFT rods with and without external thermocouples is, therefore, about 80 to 110 K.

For the 4-cm/s reflood rate of the TC-1 tests, the external cladding thermocouples induced premature quench within 3 to 12 s before the other rods. The actual time of cladding quench may also have been influenced in a similar manner in the LOFT L2 reflood. Additionally, some TC-1 surface thermocouples momentarily quenched and reheated prior to actual rod quench, a condition that may be possible in other program results. Finally, all the fuel and cladding thermocouples are considered to have performed well during the entirety of the TC-1 series. Future in-pile programs may want to consider internal rod temperature measurements in place of surface temperature measurements.

REFERENCES

1. *Code of Federal Regulations, Title 10 CFR Part 50, Appendix K*, U. S. Government Printing Office, January 1978.
2. D. L. Reeder, *LOFT System and Test Description (5.5-ft Nuclear Core 1 LOCEs)*, NUREG/CR-0247, TREE-1208, 1978.
3. United States Nuclear Regulatory Commission, Reactor Safety Program, *Description of Current and Planned Reactor Safety Research Sponsored by the Nuclear Regulatory Commission's Division of Reactor Safety Research*, NUREG-75/058, June 1975.
4. G. Class et al., *Concerning the Pretests Conducted at COSIMA for the Influence of Outside Mounted Thermocouples*, KfK Report 06.01.07P03A, PNS-Nr., August 1979, pp. 402-479.
5. R. C. Gottula, *LOFT Transient (Blowdown) Critical Heat Flux Tests*, TREE-NUREG-1240, April 1978.
6. *Halden Reactor Project Programme Proposal for the Three Year Period 1979-81*, Institutt for Atomenergi, Norway, September 1977.
7. D. J. Varacalle et al., *PBF/LOFT Lead Rod Test Series Test Results Report*, NUREG/CR-1538, EGG-2047, July 1980.

CONTENTS

APPENDIX A--ADDITIONAL PLOTS FOR TESTS TC-1B, TC-1C AND TC-1D	37
APPENDIX B--THERMAL-HYDRAULIC DATA RELATED TO TC-1 TESTS	71
APPENDIX C--FUEL ROD CHARACTERIZATION	79
APPENDIX D--EXPERIMENT DESIGN AND CONDUCT	87

FIGURES

A-1. Test TC-1B cold leg depressurization	39
A-2. Fuel rod flow shroud outlet volumetric flows of Rods 01, 02, and 03 during Test TC-1B	39
A-3. Fuel rod flow shroud inlet volumetric flows during Test TC-1B	40
A-4. Rod 01 internal rod temperatures during Test TC-1B	40
A-5. Rod 01 internal rod temperatures during blowdown phase of Test TC-1B	41
A-6. Rod 01 internal rod temperatures during reflood phase of Test TC-1B	41
A-7. Rod 02 internal rod and cladding surface temperatures, and axial extension during Test TC-1B	42
A-8. Rod 02 internal rod and cladding surface temperatures, and axial extension during blowdown phase of Test TC-1B	42
A-9. Rod 02 internal rod and cladding surface temperatures, and axial extension during reflood phase of Test TC-1B	43
A-10. Rod 03 internal rod and cladding surface temperatures, and axial extension during Test TC-1B	43
A-11. Rod 03 internal rod and cladding surface temperatures, and axial extension during blowdown phase of Test TC-1B	44
A-12. Rod 03 internal rod and cladding surface temperatures, and axial extension during reflood phase of Test TC-1B	44
A-13. Rod 04 internal rod and cladding surface temperatures, and axial extension during Test TC-1B	45
A-14. Rod 04 internal rod temperatures and axial extension during blowdown phase of Test TC-1B	45

A-15.	Rod 04 internal rod temperatures and axial extension during reflood phase of Test TC-1B	46
A-16.	Comparison of internal fuel temperatures of Rods 01 and 03 during Test TC-1B	46
A-17.	Comparison of internal fuel temperatures of Rods 03 and 04 during Test TC-1B	47
A-18.	Comparison of Rod 01 internal fuel and cladding temperatures during Test TC-1B	47
A-19.	Comparison of Rod 02 internal fuel and cladding temperatures during Test TC-1B	48
A-20.	Comparison of Rod 03 internal fuel temperatures during Test TC-1B	48
A-21.	Comparison of Rod 04 internal fuel temperatures during Test TC-1B	49
A-22.	Test TC-1C cold leg depressurization	49
A-23.	Fuel rod flow shroud outlet volumetric flows of Rods 01, 02, and 03 during Test TC-1C	50
A-24.	Fuel rod flow shroud inlet volumetric flows during Test TC-1C	50
A-25.	Rod 01 internal rod temperatures and axial extension during Test TC-1C	51
A-26.	Rod 01 internal rod temperatures and axial extension during blowdown phase of Test TC-1C	51
A-27.	Rod 01 internal rod temperatures and axial extension during Test TC-1C	52
A-28.	Rod 02 internal rod and cladding surface temperatures, and axial extension during Test TC-1C	52
A-29.	Rod 02 internal rod and cladding surface temperatures, and axial extension during reflood of Test TC-1C	53
A-30.	Rod 02 internal rod and cladding surface temperatures, and axial extension during Test TC-1C	53
A-31.	Rod 03 internal rod and cladding surface temperatures, and axial extension during blowdown phase of Test TC-1C	54
A-32.	Rod 03 internal rod and cladding surface temperatures, and axial extension during reflood phase of Test TC-1C	54

A-33.	Rod 04 internal rod and cladding surface temperatures, and axial extension during Test TC-1C	55
A-34.	Rod 04 internal rod temperatures and axial extension during blowdown phase of Test TC-1C	55
A-35.	Rod 04 internal rod temperatures and axial extension during blowdown phase of Test TC-1C	56
A-36.	Comparison of internal rod temperatures and axial extension during reflood phase of Test TC-1C	56
A-37.	Comparison of internal fuel temperatures of Rods 01 and 03 during Test TC-1C	57
A-38.	Comparison of internal fuel temperatures of Rods 03 and 04 during Test TC-1C	57
A-39.	Comparison of Rod 01 internal fuel and cladding temperatures during Test TC-1C	58
A-40.	Comparison of Rod 02 internal fuel and cladding temperatures during Test TC-1C	58
A-41.	Comparison of Rod 03 internal fuel temperatures during Test TC-1C	59
A-42.	Comparison of Rod 04 internal fuel temperatures during Test TC-1C	59
A-43.	Test TC-1D cold leg depressurization	60
A-44.	Fuel rod flow shroud outlet volumetric flows of Rods 01, 02, and 03 during Test TC-1D	60
A-45.	Fuel rod flow shroud inlet volumetric flows during Test TC-1D	61
A-46.	Rod 01 internal rod temperatures and axial extension during Test TC-1D	61
A-47.	Rod 01 internal rod temperatures and axial extension during blowdown phase of Test TC-1D	62
A-48.	Rod 01 internal rod temperatures and axial extension during reflood phase of Test TC-1D	62
A-49.	Rod 02 internal rod and cladding surface temperatures, and axial extension during Test TC-1D	63
A-50.	Rod 02 internal rod and cladding surface temperatures, and axial extension during blowdown phase of Test TC-1D	63

A-51.	Rod 02 internal rod and cladding surface temperatures, and axial extension during reflood phase of Test TC-1D	64
A-52.	Rod 03 internal rod and cladding surface temperatures, and axial extension during Test TC-1D	64
A-53.	Rod 03 internal rod and cladding surface temperatures, and axial extension during blowdown phase of Test TC-1D	65
A-54.	Rod 03 internal rod and cladding surface temperatures, and axial extension during reflood phase of Test TC-1D	65
A-55.	Rod 04 internal rod temperatures and axial extension during Test TC-1D	66
A-56.	Rod 04 internal rod temperatures and axial extension during blowdown phase of Test TC-1D	66
A-57.	Rod 04 internal rod temperatures and axial extension during reflood phase of Test TC-1D	67
A-58.	Comparison of internal fuel temperatures of Rods 01 and 03 during Test TC-1D	67
A-59.	Comparison of internal fuel temperatures of Rods 03 and 04 during Test TC-1D	68
A-60.	Comparison of Rod 01 internal fuel and cladding temperatures during Test TC-1D	68
A-61.	Comparison of Rod 02 internal fuel and cladding temperatures during Test TC-1D	69
A-62.	Comparison of Rod 03 internal fuel temperatures during Test TC-1D	69
A-63.	Comparison of Rod 04 internal fuel temperatures during Test TC-1D	70
B-1.	Typical rod peak power history during Test TC-1	74
B-2.	TC-1 Test Series power profile	74
B-3.	Total heat transfer coefficient as a function of time	75
B-4.	Coolant pressure response during the TC-1 Test Series transient phase	75
B-5.	Fuel rod flow shroud inlet and outlet coolant temperature history during Test TC-1A	76

B-6.	Fuel rod flow shroud inlet and outlet coolant temperature history during Test TC-1B	76
B-7.	Fuel rod flow shroud inlet and outlet coolant temperature history during Test TC-1C	77
B-8.	Fuel rod flow shroud inlet and outlet coolant temperature history during Test TC-1D	77
D-1.	TC-1 test train orientation	91
D-2.	TC-1 fuel rod dimensions	93
D-3.	TC-1 test train assembly	94
D-4.	PBF LOCA test system illustration	96
D-5.	Axially averaged rod power (average of the four test rods) during preconditioning and decay heat buildup of Test TC-1A	99
D-6.	Axially averaged rod power (average of the four test rods) during decay heat buildup of Tests TC-1B, TC-1C, and TC-1D	100
D-7.	Axially averaged rod power (average of the four test rods) during TC-1 transients	104

TABLES

C-1.	Composite powder analysis summary	83
C-2.	Fuel pellet and stack dimensions	84
C-3.	Fuel rod and flow shroud dimensions	85
D-1.	TC-1 fuel rod design characteristics	90
D-2.	TC-1 blowdown nozzle throat diameters and locations	97
D-3.	Coolant conditions prior to each blowdown	101
D-4.	Test rod power prior to blowdown	102
D-5.	Blowdown valve closing and opening times	104
D-6.	TC-1 posttest nitrogen leak check	106
D-7.	TC-1 posttest water leak check	107

EG&G Idaho, Inc.
P.O. Box 1625
Idaho Falls, Idaho 83415